Cell wall integrity modulates *HOOKLESS1* and *PHYTOCHROME INTERACTING FACTOR4* expression controlling apical hook formation

Riccardo Lorrai[1], Özer Erguvan[2], Sara Raggi[2], Kristoffer Jonsson[3], Jitka Široká[4], Danuše Tarkowská[4], Ondřej Novák[4], Jayne Griffiths[5], Alexander M. Jones[5], Stéphane Verger[2, 6], Stéphanie Robert[2] and Simone Ferrari[1,*]

[1] Dipartimento di Biologia e biotecnologie “Charles Darwin”, Sapienza Università di Roma, Rome, Italy

[2] Umeå Plant Science Centre (UPSC), Department of Forest Genetics and Plant Physiology, Swedish University of Agricultural Sciences, 901 83 Umeå, Sweden

[3] IRBV, Department of Biological Sciences, University of Montreal, Montreal, Quebec, Canada

[4] Laboratory of Growth Regulators, Institute of Experimental Botany, Czech Academy of Sciences and Faculty of Science, Palacký University Olomouc, CZ-78371 Olomouc, Czech Republic

[5] Sainsbury Laboratory, University of Cambridge, Cambridge, United Kingdom

[6] Umeå Plant Science Centre (UPSC), Department of Plant Physiology, Umeå University, 901 87 Umeå, Sweden

*Corresponding author:
Simone Ferrari, e-mail: simone.ferrari@uniroma1.it

The author responsible for distribution of materials integral to the findings presented in this article in accordance with the policy described in the Instructions for Authors (https://academic.oup.com/plphys/pages/General-Instructions) is Simone Ferrari.

Running head: Loss of CWI represses apical hook formation

Abstract

Formation of the apical hook in etiolated dicot seedlings results from differential growth in the hypocotyl apex and is tightly controlled by environmental cues and hormones, among which auxin and gibberellins (GAs) play an important role. Cell expansion is tightly regulated by the cell wall, but whether and how feedback from this structure contributes to hook development is still unclear. Here, we show that etiolated seedlings of the Arabidopsis (*Arabidopsis thaliana*) *quasimodo2-1* (*qua2*) mutant, defective in pectin biosynthesis, display severe defects in apical hook formation and maintenance, accompanied by loss of asymmetric auxin maxima and of differential cell expansion. Moreover, *qua2* seedlings show reduced expression of *HOOKLESS 1* (*HLS1*) and *PHYTOCHROME INTERACTING FACTOR 4* (*PIF4*), which are positive regulators of hook formation. Treatment of wild-type seedlings with the cellulose inhibitor isoxaben (isx) also prevents hook development and represses *HLS1* and *PIF4* expression. Exogenous GAs, loss of DELLA proteins or *HLS1* overexpression partially restore hook development in *qua2* and isx-treated seedlings. Interestingly, increased agar concentration in the medium restores, both in *qua2* and isx-treated seedlings, hook formation, asymmetric auxin maxima and *PIF4* and *HLS1* expression. Analysis of plants expressing a FRET-based GA sensor indicate that isx reduces accumulation of GAs in the apical hook region in a turgor-dependent manner. Lack of the cell wall integrity sensor THESEUS 1, which modulates turgor loss point, restores hook formation in *qua2* and isx-treated seedlings. We propose that turgor-dependent signals link changes in cell wall integrity to the PIF4-HLS1 signalling module to control differential cell elongation during hook formation.

Introduction

Etiolated seedlings of dicots form an apical hook to protect the meristems during soil emergence. Apical hook formation depends on the differential cell elongation on the opposite sides of the hypocotyl apex, causing the shoot to bend by 180° (Guzmán and Ecker, 1990; Abbas et al., 2013). Like most plant developmental processes, hook formation is largely controlled by phytohormones including auxin (Abbas et al., 2013). Shortly after germination, the formation of an auxin response maximum restrains cell expansion on the concave side of the hook, leading to differential cell elongation and eventually shoot bending (Abbas et al., 2013). In Arabidopsis (*Arabidopsis thaliana*), hook formation is positively controlled by the master regulator HOOKLESS 1 (HLS1) (Guzmán and Ecker, 1990; Lehman et al., 1996; Li et al., 2004; Zhang et al., 2018). HLS1 was reported to promote the asymmetric distribution of auxin between the concave and convex sides of the hypocotyl (Lehman et al., 1996) and to reduce the levels of AUXIN RESPONSE FACTOR 2 (ARF2), a repressor of auxin responses (Li et al., 2004). Both apical hook formation and *HLS1* expression are promoted by ethylene and gibberellins (GAs) (Lehman et al., 1996; An et al., 2012) and negatively regulated by jasmonates (Song et al., 2014). Regulation of hook formation by GAs is mediated by the degradation of the key repressors DELLA proteins (Sun, 2008). When GA levels are low, DELLAs promote the proteasome-mediated degradation of PHYTOCHROME INTERACTING FACTORS (PIFs) (Li et al., 2016), a family of transcription factors that positively regulate the expression of *HLS1* (Zhang et al., 2018). In addition, DELLAs inhibit the activity of PIFs by sequestering their DNA-recognition domain (Feng et al., 2008; de Lucas et al., 2008). On the other hand, jasmonates can repress hook formation by reducing *HLS1* expression (Zhang et al., 2014) and by repressing PIF function (Zhang et al., 2018). While hormonal signals coordinate hook development, their effects ultimately translate into changes in cellular properties, particularly the ability of the cell wall to yield to turgor pressure. Primary cell walls are complex and dynamic networks mainly composed of cellulose, hemicelluloses, and pectin (Cosgrove, 2005). Increasing evidence indicates that changes in plant cell wall structural polysaccharides caused either by mutations in biosynthetic genes or by chemicals, like the cellulose inhibitor isx (Heim et al., 1990), impair cell wall integrity (CWI), leading to repression of cell expansion and induction of stress responses (Vaahtera et al., 2019). For instance, etiolated Arabidopsis seedlings with altered cellulose deposition display strongly reduced hypocotyl growth (Fagard et al., 2000) and accumulate high levels of jasmonates (Engelsdorf et al., 2018). Defects in pectin composition also

restrict the growth of etiolated hypocotyls. Two Arabidopsis mutants defective for genes required for homogalacturonan (HG) biosynthesis, namely *QUASIMODO1* (*QUA1*), encoding a putative glycosyltransferase (Bouton et al., 2002), and *QUASIMODO2*/*TUMOROUS SHOOT DEVELOPMENT 2* (*QUA2*/*TSD2*), encoding a Golgi-localized pectin methyltransferase (Krupková et al., 2007; Mouille et al., 2007; Du et al., 2020), have defects in hypocotyl epidermis cell elongation and cell-to-cell adhesion (Krupková et al., 2007; Mouille et al., 2007; Raggi et al., 2015).

The molecular mechanisms regulating responses triggered by loss of CWI are only partly understood. Several responses triggered by cellulose alterations appear to be mediated by THESEUS 1 (THE1), a member of the *Catharanthus roseus* RLK1-like family of receptor-like kinases (Hématy et al., 2007; Engelsdorf et al., 2018). Perception of changes in pectin composition and activation of downstream responses are less characterized, though the FERONIA (FER) member of CrRLK1L family appears to be a possible sensor of pectin integrity (Feng et al., 2018; Lin et al., 2022).Turgor-sensitive processes appear to be relevant for the detection of CWI changes and the activation of downstream responses that restrict growth. For instance, several responses induced by isx are largely sensitive to osmotic manipulation by co-treatments with osmoticum (Hamann et al., 2009; Engelsdorf et al., 2018). Similarly, cell adhesion and elongation defects in *qua1* are suppressed by reducing external water potential *via* increased agar concentration in the growth medium (Verger et al., 2018).

Increasing evidence suggests that a feedback loop between auxin and cell wall composition regulates apical hook formation in Arabidopsis (Aryal et al., 2020; Baral et al., 2021; Jonsson et al., 2021). In particular, pectin composition seems to be associated to auxin response gradients and differential cell elongation during hook development (Jonsson et al., 2021). When auxin accumulates in the inner side of the hypocotyl, it promotes HG methylesterification, which correlates with a reduction in cell elongation (Jonsson et al., 2021). On the other hand, loss of asymmetric HG methylesterification in plants overexpressing a pectin methylesterase inhibitor alters the polar auxin transport machinery, disrupting the auxin gradient and resulting in a defective hook (Jonsson et al., 2021). In addition, alterations in other cell wall structural components, including cellulose (Sinclair et al., 2017; Baral et al., 2021) and xyloglucans (Aryal et al., 2020), also impair apical hook formation, suggesting that changes in various wall structural components converge into common responses that restrict differential cell elongation. However, the exact mechanisms linking CWI perception to the events that regulate hook development

are not fully elucidated. Here we report that loss of CWI represses a GA-modulated signalling module that comprises PIF4 and HLS1, resulting in a defective apical hook, and that these effects are suppressed by reduction of turgor pressure caused by low extracellular water potential. Our results suggest that turgor-dependent responses to altered CWI directly modulate signalling events that control differential cell expansion during hook formation.

Results

Defects in pectin biosynthesis impair hook formation and maintenance in a turgor-dependent manner

Apical hook formation was examined in a panel of Arabidopsis mutants impaired in different cell wall polysaccharides to determine the relative impact of changes in specific wall components on this process. Under our experimental conditions, three days after germination, etiolated WT seedlings displayed a completely closed hook (Fig. 1A-B), which, in contrast, was completely open in *qua2-1* (henceforth, *qua2*) as well as in two other mutants affected in pectin composition, *gae1 gae6* and *murus1* (*mur1*) (Fig. 1A-B). The *gae1 gae6* double mutant carries mutations in two glucuronate 4-epimerases (GAEs) required for the biosynthesis of UDP-D-galacturonic acid (Mølhøj et al., 2004) and is defective in HG (like *qua2*) and, possibly, rhamnogalacturonan I (RG-I) biosynthesis (Bethke et al., 2016), while *mur1* is impaired in fucose biosynthesis (Bonin et al., 1997) and has therefore defective RG-II, xyloglucans and cell wall glycoproteins (Reiter et al., 1993; Rayon et al., 1999; Freshour et al., 2003). In contrast, no significant difference in hook formation was observed in other cell wall mutants, namely *korrigan1* (*kor1*), impaired in primary cell wall cellulose deposition (Nicol et al., 1998), and *mur4* and *mur7* (Fig. 1A-B), impaired in the biosynthesis of arabinose (Reiter et al., 1997; Burget et al., 2003), with the exception of *procuste1* (*prc1*) (Desnos et al., 1996), that showed only a mild defect (Fig. 1A-B). Taken together, these results suggest that mutations in genes involved in HG biosynthesis have a major impact on hook formation, compared to genetic defects affecting other wall components.

Turgor pressure affects the activation of several responses triggered by loss of CWI (Hamann et al., 2009; Engelsdorf et al., 2018). To verify if turgor-dependent responses mediate the effects of altered pectin composition on hook formation and to determine what phases of this process are specifically affected, kinematic analysis was performed in WT, *qua2*, *gae1gae6* and *mur1* seedlings grown in the dark on medium containing 0.8% (w/v)

or 2.5% (w/v) agar [henceforth indicated as low agar (LA) and high agar (HA), respectively]. This method has been previously implemented to modulate turgor pressure in a controlled manner (Verger et al., 2018). WT seedlings grown on LA displayed typical hook development (Abbas et al., 2013), consisting in a formation phase, in which seedlings emerge from the seed and the hook angle reaches roughly 180° before 24 h after germination, followed by a maintenance phase, in which the hook is kept closed for about 48 hours, and culminating in the opening phase, in which the hook opens reaching an angle of 0° (Fig. 2A-C). In contrast, all mutants grown on LA showed a formation phase comparable, in length, to the WT, but were unable to form a fully closed hook (Fig. 2A-C). Moreover, the maintenance phase was deeply compromised in all mutants, leading to hook opening right after the maximum curvature was achieved (Fig. 2A-C).

When WT seedlings were grown on HA, formation and maintenance of the hook were largely unaffected, though the opening phase was accelerated (Fig. 2A-C). Notably, growth on HA partially restored hook formation in all mutant lines (Fig. 2A-C), leading to a significant increase in the maximum angle of curvature (Supplementary Fig. S1). In addition, HA also rescued the maintenance phase in *mur1* seedlings (Fig. 2B). Hook development could also be restored by sorbitol, an osmolyte previously shown to suppress other responses induced by cell wall damage (Hamann et al., 2009; Engelsdorf et al., 2018) (Supplementary Fig. S2). Taken together, these results indicate that the hook formation in seedlings with altered pectin composition is rescued under conditions that reduce turgor pressure.

Loss of pectin integrity disrupts differential cell expansion and asymmetric auxin response during apical hook development

Hook formation is thought to be largely dependent on the differential elongation rate of epidermal cell on the two sides of the hypocotyl (Silk and Erickson, 1978). Defects in *QUA2* restrict cell expansion in the epidermis of adult leaves (Raggi et al., 2015), suggesting that alterations in cell expansion rates might also occur in the epidermis of the hypocotyl of etiolated seedlings with altered pectin composition, resulting in a defective hook. Individual cell elongation rates were therefore measured in the apical portion of the hook of WT and, as illustrative of loss of pectin integrity, *qua2* seedlings grown in the dark in LA and HA condition. As expected, cell expansion rate in WT seedlings was lower on the inner side than on the outer side of the hypocotyl, either in LA or HA condition (Fig. 3A-

B). In contrast, *qua2* seedlings showed a significant reduction in the expansion rate in the outer side of the hook when grown on LA, but not on HA (Fig. 3A-B).

As differential cell expansion is dependent on the establishment of an auxin gradient at the two sides of the apex (Abbas et al., 2013), the distribution of auxin response was evaluated in WT and *qua2* seedlings expressing the auxin response reporter *DR5*-VENUS-NLS (Heisler et al., 2005). WT seedlings displayed a strong fluorescent signal predominantly in the inner epidermal cells of the hook, and this pattern was not affected by the agar concentration in the medium (Fig. 3C). In contrast, reporter expression was equally distributed on both sides of the hypocotyl of *qua2* seedlings grown in LA (Fig. 3C). This alteration was fully restored when the mutant was grown on HA (Fig. 3C). Taken together, our results indicate that turgor-dependent responses to altered HG hinder proper asymmetric auxin signalling gradient and differential cell expansion during hook formation.

Loss of pectin integrity represses *HLS1* and *PIF4* expression and alters the expression of genes involved in GA homeostasis

HLS1 combines upstream stimuli important for hook formation (Guzmán and Ecker, 1990), negatively regulating ARF2 levels (Li et al., 2004) and influencing auxin distribution (Lehman et al., 1996). Hook formation is also positively modulated by PIFs, and, in particular, PIF4, which directly binds to the promoter of *HLS1* to activate its transcription (Zhang et al., 2018). We therefore evaluated if a defective pectin composition might affect the expression of the genes encoding these proteins. In *qua2* seedlings grown under LA conditions *PIF4* transcript levels were sharply reduced, compared to the wild type, but increased to levels comparable to the WT under HA conditions (Fig. 4A). Consistently, *qua2* seedlings transformed with a HA-tagged version of PIF4 under the control of its native promoter (Zhang et al., 2017) displayed, under LA conditions, reduced levels of protein, that strongly increased and reached levels comparable to the wild type when seedlings were grown in HA (Fig. 4B). Transcript levels of *HLS1* were also significantly reduced in etiolated *qua2* seedlings grown in LA, in comparison to the wild type, and significantly increased in both genotypes under HA conditions (Fig. 4C). These results suggest that reduced expression of *HLS1* might impair proper hook formation in *qua2*, and that its increased expression under HA conditions might restore it. Consistently, two-day-old *qua*2 seedlings expressing a myc-tagged version of HLS1 under the control of the constitutive CaMV 35S promoter (Shen et al., 2016) and grown under LA conditions displayed significantly greater hook angle than untransformed mutant seedlings (Fig. 4D).

Hook formation and *HLS1* expression are both positively regulated by GAs (An et al., 2012). We therefore evaluated if loss of pectin integrity might affect the expression of genes involved in the homeostasis of these hormones. Etiolated *qua2* seedlings grown on LA showed reduced transcript levels for *GA20ox1* and *GA3ox1*, required for GA biosynthesis (Hedden and Phillips, 2000) (Fig. 5A, B), and increased expression of *GA2ox2*, involved in GA catabolism (Hedden and Phillips, 2000) (Fig. 5C). In contrast, under HA conditions, expression of these genes in WT and *qua2* seedlings was comparable (Fig. 5A-C). Furthermore, exogenous GAs restored almost WT-like hook formation in *qua2* mutants grown on LA (Fig. 5D). Consistently, loss of all Arabidopsis *DELLA* genes (Feng et al., 2008) in the *qua2* background partially restored hook formation (Fig. 5E). Taken together, these results suggest that responses triggered by loss of pectin integrity, and dependent on turgor pressure, repress the GA-dependent PIF4-HLS1 signalling module, hindering proper hook formation.

Isoxaben inhibits hook formation and represses *HLS1* and *PIF4* expression and GA accumulation in a turgor-dependent manner

Our results indicate that defects in pectin composition caused by the *qua2* mutation induce responses dependent on turgor pressure that suppress GA-dependent signalling events important for hook formation. As *prc1*, impaired in the cellulose synthase CESA6 (Desnos et al., 1996), show a partially defective hook (Fig. 1), we hypothesized that also defects in cellulose might have the same effects. To verify this hypothesis, a pharmacological approach was adopted, growing etiolated WT seedlings in the presence of isx, which targets cellulose synthases, including CESA6 (Desprez et al., 2002). Under LA conditions, at two days after germination, seedlings grown in the presence of isx at concentrations equal to or higher than 2.5 nM showed strongly reduced hook curvature (Fig. 6A-B). HA conditions restored hook formation in the presence of isx at a dose of 2.5 nM and, to a lesser extent, 5.0 nM (Fig. 6A-B). Analysis of WT seedlings expressing *DR5*-VENUS-NLS showed that, as observed in *qua2*, isx disrupted asymmetric auxin distribution in LA, but not in HA conditions (Fig. 6C). Consistently, in the presence of isx, cells on the outer side of the hook region of the hypocotyl showed a significant decrease in expansion rate, compared to control seedlings, only in LA, but not in HA conditions (Fig. 6D-E). Overall, these data suggest that, as observed in *qua2*, also defects in cellulose deposition impair hook formation, disturbing the formation of an auxin asymmetric distribution and repressing cell elongation on the outer side of the hook.

Furthermore, as in *qua2*, isx repressed the expression of *HLS1* under LA, but not HA conditions (Fig. 7A). Notably, overexpression of a myc-tagged version of HLS1 in *hls1-1* seedlings (Shen et al., 2016) was sufficient to restore a fully closed hook in the presence of 2.5 nM isx (Fig. 7B). Treatments with isx also reduced *PIF4* transcript accumulation under LA, but not HA conditions (Fig. 7C). Consistently, isx repressed accumulation of PIF4 protein in a dose dependent manner, but this effect was reduced under HA conditions (Fig. 7D). As observed in *qua2* seedlings, the expression of the biosynthetic *GA3ox1* and *GA20ox1* was repressed in plants treated with isx only in LA conditions, whereas expression in mock- and isx-treated seedlings was comparable in HA conditions (Supplementary Fig. S3A-C). Moreover, exogenous GAs partially restored hook formation in seedlings treated with isx (Fig. 8A). Hook formation in both the pentuple *della* mutant and in a *ga2ox* heptuple mutant, impaired in the GA catabolic GA2-oxidases GA2ox1/2/3/4/6/7/8 and therefore showing increased levels of active GAs in seedling hypocotyls (Griffiths et al., 2023), was less sensitive to isx (Fig. 8B-C), suggesting that an alteration in GA homeostasis might contribute to the inhibition of hook formation in response to loss of CWI. To further investigate this hypothesis, we analysed *in vivo* GA levels in response to isx using the FRET biosensor Gibberellin Perception Sensor 2 (GPS2) (Griffiths et al., 2023). Under LA conditions, GA levels in the hook region of the hypocotyl decreased in response to isx in a dose-dependent manner, while under HA conditions GA levels appeared to be similar in control- and isx-treated seedlings (Fig. 8D-E). These results indicate that, as in the case of *qua2*, isx downregulates GA-dependent signalling events that modulate *PIF4* and *HLS1* expression and control hook formation, suggesting a common mechanism underlying the effects of loss of CWI caused by alterations in different cell wall components on hook development.

As THE1 is a major player in the activation of responses triggered by altered cellulose deposition (Bacete and Hamann, 2020), we evaluated if this protein is also important for the inhibition of apical hook formation mediated by isx. Indeed, hook curvature in two loss-of-function *the1-1* and *the1-6* mutants (Hématy et al., 2007; Merz et al., 2017) was less sensitive to isx both in LA and HA conditions (Fig. 9A). Conversely, the gain-of-function *the1-4* mutant (Merz et al., 2017) showed increased sensitivity to isx both in HA and LA medium (Fig. 9A). Notably, both the *the1-1* and the *the1-6* mutations fully restored hook development in *qua2* seedlings (Fig. 9B). These results indicate that responses mediated by THE1 contribute to the defective hook development in plants with altered CWI.

Jasmonates are not involved in defective hook formation caused by altered cell wall integrity

Isx induces the accumulation of jasmonates in Arabidopsis seedlings in a THE1-dependent manner (Engelsdorf et al., 2018). As exogenous jasmonic acid (JA) antagonises apical hook formation in etiolated seedlings (Song et al., 2014; Zhang et al., 2014), we hypothesized that the hook defect observed in response to loss of CWI might be mediated by increased jasmonate levels. Levels of JA, jasmonyl-L-isoleucine (JA-Ile) and of the JA-derivative 11- and 12-hydroxyjasmonate (Σ 11-/ 12-OHJA, sum of unresolved 11- and 12-OHJA), were therefore quantified in dark-grown WT and *qua2* seedlings. Under LA conditions, mutant seedlings contained higher levels of all three jasmonates, compared to the wild type (Fig. 10A). Under HA conditions, the concentration of JA in WT seedlings was unaltered, while JA-Ile and Σ 11-/ 12-OHJA levels were moderately increased (Fig. 10A). Growth on HA medium significantly reduced JA and JA-Ile levels in *qua2*, while Σ 11-/ 12-OHJA concentration in the mutant was slightly increased (Fig. 10A).

To assess whether high levels of jasmonates are responsible for the altered hook formation of *qua2*, this mutant was crossed with lines defective for *JASMONATE RESISTANT 1* (*JAR1*), required for the synthesis of JA-Ile (Wasternack and Hause, 2013), or *CORONATINE INSENSITIVE 1* (*COI1*), a crucial component of the SCF COI1 E3 ubiquitin complex necessary for JA-Ile perception and transduction (Wasternack and Hause, 2013). In *qua2 coi1* seedlings, two days after germination, hook impairment was slightly exacerbated (Fig. 10B), while the *qua2 jar1* double mutant did not show differences in hook angle, compared to *qua2* (Fig. 10C). Consistently, *jar1* and *coi1* single mutants treated with isx displayed hook defects comparable to those observed in the wild type (Fig. 10D). These results indicate that, despite loss of CWI triggers the accumulation of elevated levels of jasmonates in a turgor-dependent manner, these hormones do not contribute to the observed defects in hook formation.

Taken together, our results suggest that, in plants with altered CWI, turgor-dependent responses suppress, in a THE1-dependent manner, GA-mediated downstream signalling events controlling *PIF4* and *HLS1* expression. This leads to the disruption of auxin response asymmetry, differential cell elongation and proper hook formation (Fig. 11).

Discussion

Cell wall alterations impair differential cell elongation during apical hook formation in a turgor-dependent manner

Differential cell elongation is widely used in plants to adapt growth and development to external and endogenous signals. This is exemplified by apical hook formation, which is largely dependent on the differential cell elongation on the opposite sides of the hypocotyl apex (Guzmán and Ecker, 1990; Abbas et al., 2013). Cell elongation results from the interplay between turgor pressure and cell wall elasticity and extensibility (Ray et al., 1972). It is therefore not surprising that cell wall composition has a major impact on hook formation, and that an extensive interplay occurs between cell walls and the hormonal networks controlling hook formation (Aryal et al., 2020; Jonsson et al., 2021). However, despite our considerable knowledge of the signalling pathways controlling hook development, little is known of how cell walls interact with these pathways to modulate differential cell expansion and hook bending. Here we have shown that changes in CWI, either caused by mutations in genes affecting pectin composition or by interference with cellulose deposition triggered by isx, hinder hook formation in Arabidopsis seedlings in a turgor-dependent manner. Moreover, altered CWI compromises, again in a turgor-dependent manner, asymmetric auxin maxima formation and differential cell elongation in the hook region. Additionally, turgor-mediated responses triggered by altered CWI downregulate hook-promoting signalling events that are positively regulated by GAs and include PIF4 accumulation and *HLS1* expression (Fig. 11). These results suggest that turgor pressure links CWI to GA-dependent signalling to modulate hook formation and maintenance.

Cell wall assembly and remodelling must be finely controlled during growth processes to ensure proper cell expansion while maintaining mechanical integrity (Wolf et al., 2012). Moreover, alterations in CWI can occur in response to abiotic or biotic stress (Vaahtera et al., 2019; Lorrai and Ferrari, 2021); therefore, the structural and functional integrity of the wall must be constantly monitored and fine-tuned to allow normal growth and development under physiological conditions while preventing mechanical failure under adverse conditions (Rui and Dinneny, 2020). Increasing evidence points to the role of turgor-mediated responses in triggering several effects of loss of CWI on plant growth and development (Engelsdorf et al., 2018; Verger et al., 2018). Indeed, plant cells must sustain huge turgor pressures, and their connection with each other, which is mediated by the cell

wall, allows the propagation of signals generated by turgor pressure and by differential growth (Jonsson et al., 2022). Plants with altered CWI may fail to counterbalance turgor pressure, causing mechanical stress and triggering downstream compensatory responses. Indeed, supplementation with osmolytes, like sorbitol, or increasing medium agar concentrations have been previously exploited to decrease turgor pressure and restore growth in plants with perturbed cell walls (Engelsdorf et al., 2018; Verger et al., 2018; Bacete et al., 2022). We have found that both sorbitol and HA restore hook development in plants with altered pectin composition (Fig. 2; Supplementary Fig. S1-2). Analysis of cell growth rate showed that the impaired hook formation phase observed in *qua2* or in isx-treated seedlings is accompanied by a reduction of cell elongation rate in the outer cell layer and that WT-like growth rate was restored when seedlings were grown in HA condition (Fig. 3A-B and 6D-E), further supporting the hypothesis that the compromised hook formation observed in plants with altered CWI is largely mediated by turgor-dependent mechanisms.

It has been proposed that loss of cell adhesion in plants with altered HG is a consequence of excessive tension in the epidermis caused by mechanical stress (Verger et al., 2018). Moreover, tension-mediated signals triggered by altered pectin composition might induce compensatory mechanisms that restrict cell expansion and therefore relieve mechanical stress. We have previously observed that the reduced cell expansion observed in *qua2* seedlings is at least partly mediated by an increased expression of *AtPRX71*, encoding a ROS-generating apoplastic peroxidase which is also involved in H_2O_2 production in response to isx (Raggi et al., 2015). Notably, *AtPRX71* expression is also induced by hypoosmolarity (Rouet et al., 2006), a condition leading to excessive turgor pressure. This suggests that turgor-dependent responses triggered by altered CWI might lead to compensatory mechanisms, possibly including peroxidase-mediated cell wall crosslinking, that ultimately restrict cell expansion. Such mechanisms might take place also during apical hook formation, causing the turgor-dependent defect in differential cell expansion observed in *qua2* and in isx-treated seedlings.

The observation that both the *qua2* mutation and isx impair proper hook formation under LA, but not HA conditions indicates that loss of CWI caused by alterations in either HG or cellulose trigger turgor-dependent signals that hinder differential cell expansion. However, the exact nature of these signals still needs to be clarified. It has been proposed that loss of CWI results in distortion or displacement of the plasma membrane relative to the cell wall, that can be detected by a dedicated CWI maintenance mechanism (Engelsdorf et al.,

2018). Our results suggest that THE1 plays an important role in mediating pectin- and isx-triggered inhibition of hook formation, possibly controlling the activation of responses that lead to reduced cell expansion. It has been recently proposed that THE1 might indirectly influence changes in cell wall stiffness in response to ISX/sorbitol co-treatments, possibly as a consequence of THE1 function in modulating responses to ISX (Bacete et al., 2022). Further investigation will provide insights into the role of specific components of the CWI maintenance system in modulating differential cell expansion during hook formation.

Loss of CWI represses a signalling module that promotes apical hook development

Differential elongation during hook development requires the formation of an auxin gradient, reaching a maximum on the inner side of the hook where it reduces the cell growth rate (Abbas et al., 2013). The cell wall is a key hub in this process, as a positive feedback loop mechanism couples cell wall stiffness, mediated by changes in the DM of HG with auxin redistribution (Jonsson et al., 2021). However, the mechanisms linking changes in cell wall properties and the signalling pathways that modulate differential cell expansion are poorly understood. Our results suggest that loss of CWI represses a signalling module, comprising PIF4 and HLS1, that positively regulates auxin biosynthesis and distribution and ultimately hook formation (Lehman et al., 1996; Franklin et al., 2011; Zhang et al., 2018). HLS1 suppresses the accumulation of AUXIN RESPONSE FACTOR 2 (ARF2) (Li et al., 2004), which negatively regulates hook formation and transcriptional control of auxin transporters downstream of xyloglucan defects (Aryal et al., 2020). We observed that mutants with altered pectin composition and seedlings treated with isx show a reduction of *HLS1* and *PIF4* transcript levels (Fig. 4A, C and 7A, C), and of PIF4 protein levels (Fig. 4B and 7D). The downregulation of *HLS1* and *PIF4* might contribute to the disruption of asymmetric auxin maxima and differential cell expansion observed in *qua2* and might also contribute to the hook defect caused by altered cellulose deposition, as HLS1 overexpression confers partial resistance to the inhibitory effect of isx (Fig. 7B) and of *qua2* mutation (Fig. 4D). These observations point to a common regulation of hook formation in response to changes in different cell wall components.

Mechanical stress arising from turgor pressure changes can activate JA-mediated stress responses in plants with altered CWI (Engelsdorf et al., 2018). Recently, it has been proposed that JA-Ile accumulation in the roots of the *kor1* mutant is prompted by turgor-driven mechanical compression at the level of the cortex (Mielke et al., 2021). We found that *qua2* seedlings accumulate high levels of jasmonates, which decrease when the

mutant is grown in HA conditions (Fig. 10A), confirming that cell wall stress-induced JA production is mediated by turgor pressure changes. However, JA signalling does not appear to be involved in the repression of hook development caused by loss of CWI neither in *qua2* nor in isx-treated seedlings (Fig. 10B-D). On the other hand, our results suggest that hook defects in plants with an altered cell wall might be at least partially mediated by a reduction in GA accumulation, as 1) GA levels are reduced in isx-treated seedlings (Fig. 8D-E) under LA conditions and are restored by HA; 2) both *qua2* and isx-treated WT seedlings show altered expression of genes involved in the homeostasis of GAs (Fig. 5A-C and Supplementary Fig. S3); 3) exogenous GAs restore hook formation in *qua2* and in isx-treated WT seedlings (Fig. 5D and 8A); 4) lack of DELLA or GA2ox proteins, that increase GA response or levels, respectively, reduces the impact of isx on hook formation (Fig. 8B-C). Notably, growth of seedlings on HA increases *HLS1*, *PIF4* and GA biosynthetic gene expression in both *qua2* and isx-treated seedlings (Fig. 4A, C, 5A-C, 7A, C, Supplementary Fig. S3), and overexpression of HLS1 restores hook formation in *qua2* and in isx-treated seedlings (Fig. 4D and 7B). Furthermore, HA conditions prevent the reduction of PIF4 protein levels in *qua2* and in isx-treated seedlings (Fig. 4B and 7D). These results suggest a causal link between altered CWI, reduction of GA levels and suppression of GA-mediated signalling required for proper auxin signalling and differential cell expansion during hook formation and maintenance.

In conclusion, our results indicate that turgor-dependent responses link changes in CWI to the downregulation of a regulatory module, comprising GAs, PIF4 (and, possibly, other PIFs) and HLS1, that promotes asymmetric cell elongation and hypocotyl curvature during hook formation (Fig. 11). However, it cannot be ruled out that additional mechanisms might contribute to compromise hook formation in plants with defective cell wall composition. Intriguingly, it was reported that short fragments of HG restore hook development in dark-grown mutants impaired in pectin composition (Sinclair et al., 2017), suggesting that, in WT plants, HG-derived fragments might act as signals that promote hook formation. Future research will help elucidate the mechanisms linking changes in the cell wall biochemical and physical properties occurring in response to internal and environmental cues to the signalling cascades that modulate differential cell growth during plant developmental programs.

Materials and Methods

Plant lines

All experiments were performed using Arabidopsis (*Arabidopsis thaliana*) lines. The *qua2-1* mutant was a kind gift of Gregory Mouille (INRA Centre de Versailles-Grignon); *coi1-1* and *jar1-1* mutant were a gift of Edward Farmer (Department of Plant Molecular Biology, University of Lausanne). The *mur1-1*, *mur4-1*, *mur7-1*, *prc1-1*, *kor1-1*, *gae1-1 gea6-1* mutants and the pentuple *della* mutant (*gai-t6*, *rga-t2*, *rgl1-1*, *rgl2-1* and *rgl3-1*) were obtained by the Nottingham Arabidopsis Stock Centre. The transgenic *PIF4p:PIF4-HA pif4-301* (Zhang et al., 2017) line was a kind gift of Christian Fankhauser (University of Lausanne, Center for Integrative Genomics). The 35S::Myc-HLS1/*hls1-1* line was a gift by Shangwei Zhong (Peking University). The *the1-1*, *the1-4* and *the1-6* mutants were a gift by Herman Höfte (INRA Centre de Versailles-Grignon). Generation of the *ga2oxheptuple* mutant (*ga2ox1/2/3/4/6/7/8*) is described in Griffiths et al., 2023.

The *qua2-1 coi1-1* and *qua2-1 jar1-1* double mutant lines were generated by crossing single mutants. Double homozygous lines were isolated based on the presence of cell adhesion defects in the hypocotyl and on primary root resistance to exogenous JA. *qua2-1 coi1-1* double homozygous mutants were crossed with a *qua2-1/qua2-1 coi1-1/COI1* sesquimutant, and homozygous individuals of the segregating progeny were selected based on their insensitivity to JA in terms of root elongation. The *qua2-1 the1-1* and *qua2-1 the1-6* double mutant lines were generated by crossing single mutants. Double mutants were screened for *qua2-1* homozygous mutation for the presence of cell adhesion defects in the hypocotyl, while PCR was used to identify *the1-1* and *the1-6* homozygous individuals. The *qua2-1* 35S::Myc-HLS1/*hls1-1*, *qua2-1* homozygous mutation was identified by the presence of cell adhesion defects while 35S::Myc-HLS1/*hls1-1* was isolated by PCR.

The *PIF4p:PIF4-HA pif4-301 qua2-1* line was generated by crossing. The *qua2* DR5-VENUS line was generated by crossing a wild-type (WT) line expressing DR5-VENUS (*pDR5rev::3XVENUS-N7*) (Heisler et al., 2005) with *qua2-1*. The *qua2-1* myr-YFP line, expressing the myr-YFP plasma membrane marker line, was obtained by crossing a WT line carrying the pUBQ10::myr:YFP construct (Willis et al., 2016) with a homozygous *qua2-1* line. In all cases, double *qua2-1* homozygous individuals were isolated based on the presence of cell adhesion defects in the hypocotyl, and homozygosity of the transgene was confirmed based on the F3 generation.

All lines used in this work were in the Col-0 background, except for *kor1-1*, in Wassilewskija (Ws) background, and *della*, in Landsberg erecta (Ler) background.

Plant growth conditions

Seeds were surface sterilised with absolute ethanol (v/v), air dried and sown on a solid medium containing 2.2 gL^{-1} Murashige-Skoog (MS) salts (Duchefa), 1% (w/v) Suc, 0.8% or 2.5% (w/v) plant agar (Duchefa), pH 5.6. Plates were wrapped in aluminium foil and stratified at +4°C for 2-3 days. Isx (Merck) was dissolved in 0.01% (v/v) dimethyl sulfoxide (DMSO) and supplemented to a growth medium at indicated concentrations. For etiolated growth, after stratification, germination was induced by exposure to white light for 4-6 hours, plates were wrapped in aluminium foils and placed in a growth chamber for the indicated days. Images of the apical hook were acquired with an optical microscope using 5x magnification with light from below the sample at the indicated time after germination. For hook angle analysis with sorbitol supplementation, seeds were sown on a sterilised nylon mesh placed on agar medium plates without sorbitol and placed in the dark as described above. After 24 h, the nylon mesh was transferred under a green dim light to new plates containing sorbitol. All supplements were added in the indicated concentrations to autoclaved control media. For RNA and protein analysis, seedlings were harvested under dim green light and flash-frozen in liquid nitrogen.

Kinematic analysis of apical hook development and cell elongation measurement

Seedlings were grown vertically on solid medium plates in the dark at 21°C, illuminated with far infra-red light (940 nm). Seedlings were photographed every hour using a Raspberry Pi camera (www.raspberrypi.com). Apical hook angles were measured using Image J software (http://imagej.nih.gov/ij/).

For time-lapse imaging of cell expansion, WT myr-YFP and *qua2-1* myr-YFP seedlings were imaged using a Zeiss LSM800 confocal microscope equipped with 10x/0.45 Plan-apo dry objective. Z-stacks were acquired without averaging with a 0. 62-micron cubic voxel size. YFP excitation was performed at 525 nm wavelength (laser intensity between 1-3.2%) and the emission was collected at 400–650 nm for (donor emission), gain between 620-650.Dark-grown seedlings were placed on an agar gel block on a microscopy slide and imaged at three-hour intervals. Between the acquisition of images, seedlings were placed vertically in a dark chamber to maintain skotomorphogenic conditions. Cell elongation was calculated using the software MorphographX (MGX). Using MGX,

epidermal cell surface area from Z-stacks was extracted as described previously (Barbier de Reuille et al., 2015). The longitudinal expansion was calculated in MGX by overlaying Z-stacks with a fitted curved Bezier grid providing axial growth coordinates. For each condition and genotype, 15 cells from both the inner and the outer side of the hook were measured from each of nine individual seedlings (135 cells). The data was statistically analysed by two-tailed Student's t-test.

Gene expression analysis

To analyse gene expression, the uppermost part of seedling hypocotyls, including the apical hook, was isolated using a razor blade, frozen in liquid nitrogen and homogenised with an MM301 Ball Mill (Retsch, Germany) mixer ill for about 1 min at 25Hz. Total RNA was extracted with NucleoZOL reagent (Macherey-Nagel, Germany) according to the manufacturer's instructions. 1 µg of total RNA was retrotranscribed with Improm II Reverse Transcriptase (Promega, USA). cDNA was mixed with iTaq Universal SYBR Green Supermix (Bio-Rad) and amplified using a CFX96 Real-time System (Bio-Rad, USA) using primer pairs specific for the genes of interest (Supplementary Table S1). Expression levels of each gene, relative to the *UBIQUITIN5* (*UBQ5*), were determined using a modification of the Pfaffl method (Pfaffl, 2001) as previously described (Ferrari et al., 2006).

Protein extraction and immunoblot assays

Total proteins were extracted from etiolated seedlings (n=30) grounded in liquid nitrogen and resuspended in 120 µL of extraction buffer [125 mM Tris, pH 6.8, 4% (w/v) SDS, 20% (v/v) glycerol, 0.02% (w/v) bromophenol blue, 10% (v/v) β-mercaptoethanol]. Samples were heated for 5 min at 95°C and centrifuged for 1 min at 15,000×g at room temperature. Proteins (20 µL of each sample) were separated by 8% (v/v) acrylamide SDS-PAGE and transferred to a nitrocellulose membrane using the Trans-Blot Turbo transfer kit (Bio-Rad, USA). 5% (w/v) milk dissolved in phosphate-buffered saline with 0.05% (v/v) Tween 20 (Sigma) was used for blocking for 1.5 h at room temperature and antibody dilutions. For the detection of HA, a 1:1000 dilution of the (F-7) sc-7392 antibody (Santa Cruz Biotechnology, USA) was used. As a secondary antibody, a 1:2000 dilution of horseradish peroxidase- (HRP-) conjugated anti-mouse immunoglobulin (Cell Signaling Technology, USA) was used. An anti-actin polyclonal primary antibody (Agrisera) was used as a loading control, with HRP-conjugated anti-rabbit immunoglobulin (1:2000; Cell Signaling) as a secondary antibody. The chemiluminescent signal of HRP conjugated to secondary

antibodies was detected with ECL Western Blotting Substrate (Promega, USA) using a ChemiDoc XRS+ system (Bio-Rad, USA).

Confocal laser-scanning microscopy

For DR5::VENUS detection, two days after germination, etiolated seedlings were placed between a microscopy slide and a cover slip. Images were acquired using a Zeiss LSM 880 laser scanning confocal microscope, using the Zen black software, with a 20X (C-Apochromat 20x/1.2 W Korr FCS M27) objective. Z-stacks were acquired without averaging with the image size 1024x1024 px and 0.345-micron pixel size and a Z-step size of 1µm. VENUS excitation was performed at 514 nm wavelength (laser intensity 1%) and the emission was collected in the 518-560 nm range, gain 600. The laser reflection was filtered by a beam splitter.

For *in vivo* GA analysis, one day after germination dark-grown seedlings were mounted in liquid ¼ x MS medium [1/4 X MS salts, 0.025% (w/v) MES, pH5.7], covered with a coverslip and the entire hypocotyl was imaged. Confocal images were acquired with a format of 1024×1024 pixels and a resolution of 12 bit on an upright Leica SP8-iPhox using a 20x dry objective. For FRET analysis, the same settings described in (Rizza et al., 2017) were applied. The three fluorescence channels collected for FRET imaging were: Cerulean donor excitation and emission or DxDm, Cerulean (CFP) donor excitation, Aphrodite (YFP) acceptor emission or DxAm, and Aphrodite acceptor excitation and emission or AxAm. CFP excitation was performed at 448 nm wavelength (laser intensity 5%) and the emission was collected at 460–500 nm for CFP (donor emission) and 525–560 nm for YFP (FRET emission), gain 110. For segmentation, YFP excitation was performed at 514 nm wavelength (laser intensity 3%) and the emission was collected at 525–560 nm, gain 110. Imaging processing and analysis were performed with FRETENATOR plugins (Rowe et al., 2022; Rowe et al., 2023). The AxAm channel was used for segmentation. For segmentation Otsu thresholds were used, a difference of Gaussian kernel size was determined empirically, and a minimum ROI size was set to 20. Distance from meristem was defined using FRETENATOR ROI labeller.

Jasmonate quantification

For hormone level determination, dark-grown seedlings were harvested two days after germination, homogenised with mortar and pestle in liquid nitrogen and reweighted into three replicates (approximately 10 mg per sample). Analysis of jasmonates was performed

following a previously described protocol (Floková et al., 2014). Briefly, the samples were extracted in 1 mL of ice-cold 10% (v/v) aqueous methanol with the addition of isotopically labelled internal standards (JA-d_6 and JA-d_2-Ile, purchased from OlChemIm, Czech Republic) and the resulting extracts were purified on Oasis® HLB SPE columns (1 cc/30 mg, Waters, Milford, MA, USA). The analyses were carried out using a 1290 Infinity liquid chromatography system coupled to an Agilent 6490 Triple Quadrupole mass spectrometer (Agilent Technologies, Santa Clara, CA, USA). The data were processed in MassHunter Quantitative B.09.00 software (Agilent Technologies, Santa Clara, CA, USA) (Agilent Technologies, Santa Clara, CA, USA) (Široká et al., 2022).

Accession Numbers

The Arabidopsis Genome Initiative numbers for the genes mentioned in this article are as follows: AT1G78240 (*QUA2*); AT4G37580 (*HLS1*); AT2G43010 (*PIF4*); AT1G15550 (*GA3ox1*); AT4G25420 (*GA20ox1*); AT3G51160 (*MUR1*); AT1G30620 (*MUR4*); AT4G30440 (GAE1); AT3G23820 (*GAE6*); AT5G64740 (PRC1); AT5G49720 (*KOR1*); AT2G46370 (*JAR1*); AT2G39940 (*COI1*); AT2G01570 (*RGA*); AT1G14920 (*GAI*); AT1G66350 (*RGL1*); AT3G03450 (*RGL2*); AT5G17490 (*RGL3*); AT1G78440 (*GA2OX1*); AT1G30040 (*GA2OX2*); AT2G34555 (*GA2OX3*); AT1G47990 (*GA2OX4*); AT1G02400 (*GA2OX6*); AT1G50960 (*GA2OX7*); AT4G21200 (*GA2OX8*); AT5G54380 (*THE1*).

Supplementary Data

Supplementary Figure S1. Apical hook angle in pectin mutants grown on low and high agar.

Supplementary Figure S2. Osmotic support suppresses apical hook defects in pectin mutants.

Supplementary Figure S3. Effects of isoxaben on the expression of genes involved in GA metabolism.

Supplementary Table S1. Primers used for RT-qPCR analysis and genotyping.

Funding

This work was supported by Sapienza University of Rome (“Progetti di Avvio alla Ricerca 2021 – Tipo 2” grant n. AR22117A5E76C7EE, awarded to R.L.; "Progetti di Ricerca 2021 -

Progetti Medi" grant n. RM12218161B8A750 and Progetti di Ricerca 2019 - Progetti Medi" grant n. RM11916B6F156C03, awarded to S.F.) and by Regione Lazio (grant n. A0375-2020-36720 “Alternative use of agri-food waste in a circular economy context”, call Lazioinnova for Research Group Projects 2020, awarded to S.F.). This work was also supported by grants from the Knut and Alice Wallenberg Foundation (KAW 2016.0341, KAW 2016.0352 and KAW 2022.0029 (SaR)), the Swedish Governmental Agency for Innovation Systems (VINNOVA 2016-00504) and Vetenskapsrådet VR-2020-03420 (Sa.R., S.R.). We also thank Bio4Energy, a Strategic Research Environment supported through the Swedish Government's Strategic Research Area initiative, for supporting this work. R.L. is supported by the Italian Ministry of University and Research (MUR) (project “Development of bio-based solutions for the valorisation of waste agri-food biomass”, D.M. n. 1062 -10.08.2021 PON “Ricerca e Innovazione” 2014-2020, Asse IV “Istruzione e ricerca per il recupero” – Azione IV.4 – “Dottorati e contratti di ricerca su tematiche dell’innovazione” e Azione IV.6 – “Contratti di ricerca su tematiche Green”). J.S. was financially supported by Czech Science Foundation project No. 22-17435S. J.S. and O.N. thank Miroslava Špičáková for her technical support. D.T. is grateful for the technical assistance of Renata Plotzova and for financial support from the Ministry of Education, Youth and Sports of the Czech Republic (European Regional Development Fund-Project ‘Towards Next Generation Crops’ no. CZ.02.01.01/00/22/_008/0004581).
JG and AMJ were supported by the Gatsby Charitable trust (GAT3395) and the European Research Council under the European Union’s Horizon 2020 research and innovation program (grant agreement n° 759282).
KJ was supported by an International Post-doc grant from Vetenskapsrådet (2020-06442).
This study was carried out within the Agritech National Research Center and received funding from the European Union Next-GenerationEU (PIANO NAZIONALE DI RIPRESA E RESILIENZA (PNRR) – MISSIONE 4 COMPONENTE 2, INVESTIMENTO 1.4 – D.D. 1032 17/06/2022, CN00000022). This manuscript reflects only the authors’ views and opinions, neither the European Union nor the European Commission can be considered responsible for them.

Acknowledgments

We are grateful to Christian Fankhauser (University of Lausanne) for providing *PIF4p:PIF4-HApif4-301* seeds, to Edward Farmer (University of Lausanne) for providing

coi1-1 and *jar1-1* seeds, to Shangwei Zhong (Peking University) for providing 35S:Myc-HLS1/*hls1-1* seeds. The authors acknowledge the facilities and technical assistance of the Umeå Plant Science Centre (UPSC) Microscopy facility.

Author contributions

R.L. and S.F designed the project; R.L., O.E., K.J., D.T., Sa.R., J.G. and J.S. performed experiments; R.L, S.F., S.V., S.R., A.M.J., K.J., analysed data and critically discussed results; S.F., S.V., S.R., K.J., O.N. and A.M.J. acquired the funding; R.L and S.F. wrote the manuscript together with contributions from all authors.

Conflicts of interest

The authors declare that they have no conflict of interest with this work.

Figure legends

Figure 1. Apical hook formation in Arabidopsis cell wall mutants. (**A**) Representative pictures of wild-type (WT) Columbia-0 (Col), WT Wassilewskija (Ws), *qua2*, *mur1*, *mur4*, *mur7*, *gae1gae6*, *prc1* (in Col-0 background) and *kor1* (in Ws background) three days after germination. Scale bars in all panels, 0.5 mm. (**B**) Quantification of apical hook angles of seedlings grown as in (**A**). Box plots indicate the 1st and 3rd quartiles split by median; whiskers show range (n≥20). Letters indicate statistically significant differences ($p<0.05$) according to one-way ANOVA followed by post-hoc Tukey's HSD.

Figure 2. Kinematic analysis of apical hook formation in pectin mutants grown on low and high agar. Wild-type (WT, blue and grey lines) and *qua2* (**A**), *mur1* (**B**) or *gae1gae6* (**C**) mutant (orange and yellow lines) seedlings were grown in the dark on medium containing either 0.8% (w/v) (LA, blue and orange lines) or 2.5% (w/v) agar (HA, gray and yellow lines). The hook angle was measured at the indicated times. Error bars represent mean angle ± SE (n≥15).

Figure 3. Effects of agar concentration on cell elongation and auxin response during apical hook formation in *qua2* seedlings. (**A**) Heatmaps of the growth rate of individual

cells in the apical portion of the hypocotyl upon a three-hour time lapse in wild-type (WT) and *qua2* seedlings grown in the dark on medium containing 0.8% (LA) or 2.5% (HA) (w/v) agar. (**B**) Quantification of the growth rate of individual cells in the outer (dark grey) and inner (light grey) side of the hypocotyl of seedlings grown as in (**A**). Data are average of three independent biological replicates ± SD. In violin plots, the box limits represent the 1st and 3rd quartiles split by median, whiskers show range. For each experiment, 15 cells from both the inner and outer sides of the hook were measured from each of 9 individual seedlings. Asterisks indicate statistical significance by Student's t-test (**, $p<0.01$; ***, $p<0.001$). (**C**) Representative confocal laser scanning microscopy images of WT and *qua2* seedlings expressing the DR5::Venus-NLS and grown in the dark on LA or HA. White asterisks in (**C**) mark position of SAM. Scale bars in all panels, 50 µm.

Figure 4. *HLS1* and *PIF4* expression in *qua2* mutant. Total RNA was extracted from wild-type (WT) and *qua2* seedlings two days after germination grown in the dark on medium containing 0.8% (LA) or 2.5% (HA) agar (w/v). (**A**) Expression of *PIF4* was analysed by RT-qPCR, using *UBQ5* as a reference. (**B**) Transgenic lines expressing PIF4-HA under the control of its native promoter (ProPIF4:PIF4- 3×HA) in *pif4*-101 or *qua2-1* background were grown on LA or HA medium. PIF4-HA levels were detected by immunoblot analysis with an antibody against HA; an antibody against actin (ACT) was used as a loading control. (**C**) Expression of *HLS1* was analysed by RT-qPCR, using *UBQ5* as a reference. Bars (in **A** and **C**) indicate mean of at least three independent biological replicates ± SD. Asterisks indicate statistically significant differences with WT according to Student's t-test (*, $p<0.05$), number signs indicate statistically significant differences with LA between same genotype according to Student's t-test (#, $p<0.05$). (**D**) Quantification of apical hook angles of wild-type (WT), 35S:Myc-HLS1/*hls1-1*, *qua2*, and *qua2* 35S:Myc-HLS1/*hls1-1* seedlings two days after germination grown in the dark. Box plots in (**D**) indicate the 1st and 3rd quartiles split by median; whiskers show range ($n\geq20$). Letters indicate statistically significant differences ($p<0.05$) according to one-way ANOVA followed by post-hoc Tukey's HSD.

Figure 5. Defects in the expression of GA biosynthetic genes in *qua2* mutant. Expression of *GA3ox1* (**A**), *GA20ox1* (**B**) and *GA2ox2* (**C**) in WT and *qua2* seedlings grown in LA and HA. Transcript levels were determined by RT-qPCR using *UBQ5* as a reference. Bars indicate mean of at least three independent biological replicates ± SD. Asterisks indicate statistically significant differences with WT according to Student's t-test

(*, p<0.05; **, p<0.01), number signs indicate statistically significant differences with LA between same genotype according to Student's t-test (#, p<0.05). (**D**) Apical hook angles of WT and *qua2* seedlings two days after germination grown in the dark on medium supplemented with ethanol (mock, white boxes) or 50 µM GA_4 (GA, yellow boxes). (**E**) Apical hook angles of wild-type Ler (WT), *della*, *qua2* and *qua2 della* sixtuple mutant seedlings two days after germination grown in the dark. Box plots in (**D-E**) indicate the 1st and 3rd quartiles split by median; whiskers show range (n≥20). Letters indicate statistically significant differences, according to two-way ANOVA followed by post-hoc Tukey's HSD (p<0.05).

Figure 6. Isoxaben inhibits apical hook formation in a turgor-dependent manner. (**A**) Representative pictures of wild-type (WT) seedlings two days after germination grown in the dark on medium 0.8% (LA) or 2.5% (HA) agar (w/v) and supplemented with isoxaben (isx) at the indicated doses. Scale bars in all panels, 0.5 mm. (**B**) Quantification of apical hook angles of WT seedlings grown as in (**A**). Box plots in (**B**) indicate the 1st and 3rd quartiles split by median; whiskers show range (n≥20). Letters indicate statistically significant differences, according to two-way ANOVA followed by post-hoc Tukey's HSD (p<0.05). (**C**) Representative confocal laser scanning microscopy images of WT seedlings expressing the DR5::Venus-NLS grown in the dark with 2.5 nM isx in the dark on LA or HA. White asterisks in (**C**) mark the position of SAM. Scale bars in all panels, 50 µm. (**D**) Heatmaps of the growth rate of individual cells in the apical portion of the hypocotyl upon a three-hour time lapse in wild-type (WT) grown in the dark on medium containing 0.8% (LA) or 2.5% (HA) (w/v) agar supplemented with 2.5 nM isx. (**E**) Quantification of the growth rate of individual cells in the outer (dark grey) and inner (light grey) side of the hypocotyl of seedlings grown as in (**D**). Data are average of three independent biological replicates ± SD. In violin plots, the box limits represent the 1st and 3rd quartiles split by median, whiskers show range. For each experiment, 15 cells from both the inner and outer sides of the hook were measured from each of 9 individual seedlings. Asterisks indicate statistical significance by Student's t-test (*, p<0.05; ***, p<0.001).

Figure 7. Isoxaben inhibits *PIF4* and *HLS1* expression in a turgor-dependent manner. (**A**) Expression of *HLS1* in WT seedlings two days after germination grown in the dark with 2.5 nM isx in LA and HA. Transcript levels were determined by RT-qPCR using *UBQ5* as a reference. (**B**) Quantification of apical hook angles of wild-type (WT) and 35S:Myc-HLS1/*hls1-1* seedlings two days after germination grown in the dark in the presence of the indicated concentrations of isx (WT, white boxes; 35S:Myc-HLS1/*hls1-1*,

yellow boxes). (**C**) Expression of *PIF4* in WT seedlings two days after germination grown in the dark with 2.5 nM isx in LA and HA. Transcript levels were determined by RT-qPCR using *UBQ5* as a reference. (**D**) Transgenic lines expressing PIF4-HA under the control of its native promoter (ProPIF4:PIF4-3×HA) in *pif4*-101 background were grown on LA or HA medium supplemented with the indicated concentrations of isx. PIF4-HA levels were detected by immunoblot analysis with an antibody against HA; an antibody against actin (ACT) was used as a loading control. Bars in (**A** and **C**) indicate mean of at least three independent biological replicates ± SD. Asterisks indicate statistically significant differences between mock- and isx-treated seedlings according to Student's t-test (*, $p<0.05$); number signs indicate statistically significant differences between similarly treated seedlings grown on LA or HA according to Student's t-test ($^{\#}$, $p<0.05$). Letters in (**B**) indicate statistically significant differences according to two-way ANOVA followed by post-hoc Tukey's HSD ($p<0.05$). Box plots indicate the 1st and 3rd quartiles split by median; whiskers show range ($n\geq20$).

Figure 8. Isoxaben inhibits GA accumulation and signalling in a turgor-dependent manner. (**A**) Apical hook angles of WT seedlings two days after germination grown in the dark and treated with DMSO or 2.5 nM isoxaben (isx) in the presence or absence of 50 µM GAs. (**B**) Apical hook angles of wild-type Ler (WT, white boxes) and *della* (yellow boxes) seedlings two days after germination grown in the dark in the presence of isx at the indicated doses. (**C**) Apical hook angles of wild-type Col-0 (WT, white boxes) and *GA2oxheptuple* (yellow boxes) seedlings two days after germination grown in the dark in the presence of isx at the indicated doses. (**D**) nlsGPS2 nuclear emission ratios from $n\geq8$ hypocotyls of seedlings one day after germination grown in the dark in the presence of the indicated amount of isx on medium containing 0.8% (LA) or 2.5% (HA) agar (w/v). (**E**) Representative images of nlsGPS2 emission ratios of the hypocotyls of seedlings grown as in (**D**). Letters in **(A-D)** indicate statistically significant differences according to two-way ANOVA followed by post-hoc Tukey's HSD ($p<0.05$). Box plots indicate the 1st and 3rd quartiles split by median; whiskers show range ($n\geq20$) in (**A-C**) ($n\geq12$) in (**D**). White asterisks in (**E**) mark position of SAM, scale bars in all panels, 100 µm.

Figure 9. Apical hook inhibitions by isoxaben supplementation or *qua2* mutation is dependent on THE1. (**A**) Quantification of apical hook angles of WT (Col-0), *the1-1*, *the1-6* and *the1-4* seedlings two days after germination grown in the dark on medium 0.8% (LA) or 2.5% (HA) agar (w/v) and supplemented with isoxaben (isx) at the indicated doses. (**B**)

Quantification of apical hook angles of WT, *qua2*, *the1-1*, *the1-6*, *qua2 the1-1* and *qua2 the1-6* seedlings two days after germination grown in the dark. Letters indicate statistically significant differences according to two-way ANOVA followed by post-hoc Tukey's HSD ($p<0.05$). Box plots indicate the 1st and 3rd quartiles split by median; whiskers show range ($n\geq20$).

Figure 10. Inhibition of apical hook formation in response to altered cell wall integrity is independent of jasmonate signalling. (**A**) Levels of JA, JA-Ile, Σ 11-/ 12-OHJA in wild-type (WT, white bars) and *qua2* (black bars) seedlings two days after germination grown in the dark on medium containing 0.8% (LA) or 2.5% (HA) agar (w/v). Bars represent means of three independent biological replicates ± SD. Asterisks indicate significant differences relative to WT, according to Student's t-test (*$p\leq0.05$, **$p\leq0.01$, ***$p\leq0.001$). (**B**-**C**) Apical hook angles of WT, *qua2*, *coi1* and *qua2 coi1* (**B**), or *jar1* and *qua2 jar1* (**C**) grown as in (**A**). (**D**) Quantification of apical hook angles of wild type (WT Columbia), *jar1* and *coi1* seedlings two days after germination grown in the dark in the presence of isoxaben (isx) at the indicated doses (WT, white boxes; *jar1*, grey boxes; *coi1* yellow boxes). Box plots in (**B**-**D**) indicate the 1st and 3rd quartiles split by median, and whiskers show range ($n\geq20$). Letters indicate statistically significant differences ($p<0.05$) according to two-way ANOVA followed by post-hoc Tukey's HSD.

Figure 11. Proposed model of the effects of loss of cell wall integrity on apical hook formation. Perturbation of cell wall integrity (CWI), either caused by mutations in pectin composition or by isoxaben, activates turgor-dependent responses that repress accumulation of active gibberellins (GAs), leading to stabilization of DELLA proteins and reduction of PIF4 and possibly other PIFs protein levels. Increased DELLAs and reduced PIFs result in impaired *HLS1* expression, impairing proper formation of auxin response maxima and differential cell elongation, and ultimately inhibiting apical hook development. The arrows indicate positive regulation, and blunt-ended bars indicate inhibition. Question mark indicates unidentified signalling elements. Elements in grey indicate reduction of levels or reduced downstream responses. Ψ_w, water potential; PIFs, PHYTOCHROME INTERACTING FACTORs; HLS1, HOOKLESS 1; DELLAs, DELLA proteins; GAs, gibberellins; CW, cell wall; CWI, cell wall integrity.

References

Abbas M, Alabadí D, Blázquez MA (2013) Differential growth at the apical hook: all roads lead to auxin. Frontiers in Plant Science 4:

An F, Zhang X, Zhu Z, Ji Y, He W, Jiang Z, Li M, Guo H (2012) Coordinated regulation of apical hook development by gibberellins and ethylene in etiolated Arabidopsis seedlings. Cell Res **22**: 915–927

Aryal B, Jonsson K, Baral A, Sancho-Andres G, Routier-Kierzkowska A-L, Kierzkowski D, Bhalerao RP (2020) Interplay between cell wall and auxin mediates the control of differential cell elongation during apical hook development. Current Biology **30**: 1733-1739. e3

Bacete L, Hamann T (2020) The Role of Mechanoperception in Plant Cell Wall Integrity Maintenance. Plants **9**: 574

Bacete L, Schulz J, Engelsdorf T, Bartosova Z, Vaahtera L, Yan G, Gerhold JM, Tichá T, Øvstebø C, Gigli-Bisceglia N, et al (2022) THESEUS1 modulates cell wall stiffness and abscisic acid production in Arabidopsis thaliana. Proc Natl Acad Sci U S A **119**: e2119258119

Baral A, Aryal B, Jonsson K, Morris E, Demes E, Takatani S, Verger S, Xu T, Bennett M, Hamant O, et al (2021) External Mechanical Cues Reveal a Katanin-Independent Mechanism behind Auxin-Mediated Tissue Bending in Plants. Developmental Cell **56**: 67-80.e3

Barbier de Reuille P, Routier-Kierzkowska A-L, Kierzkowski D, Bassel GW, Schüpbach T, Tauriello G, Bajpai N, Strauss S, Weber A, Kiss A, et al (2015) MorphoGraphX: A platform for quantifying morphogenesis in 4D. eLife **4**: e05864

Bethke G, Thao A, Xiong G, Li B, Soltis NE, Hatsugai N, Hillmer RA, Katagiri F, Kliebenstein DJ, Pauly M (2016) Pectin biosynthesis is critical for cell wall integrity and immunity in Arabidopsis thaliana. The Plant Cell **28**: 537–556

Bonin CP, Potter I, Vanzin GF, Reiter W-D (1997) The MUR1 gene of Arabidopsis thaliana encodes an isoform of GDP-d-mannose-4,6-dehydratase, catalyzing the first step in the de novo synthesis of GDP-l-fucose. Proceedings of the National Academy of Sciences **94**: 2085–2090

Bouton S, Leboeuf E, Mouille G, Leydecker M-T, Talbotec J, Granier F, Lahaye M, Höfte H, Truong H-N (2002) QUASIMODO1 encodes a putative membrane-bound glycosyltransferase required for normal pectin synthesis and cell adhesion in Arabidopsis. The Plant Cell **14**: 2577–2590

Burget EG, Verma R, Molhoj M, Reiter WD (2003) Molecular cloning and characterization of a golgi-localized UDP-d-xylose 4-epimerase encoded by the MUR4 gene of Arabidopsis. Plant Cell **15**: 31

Cosgrove DJ (2005) Growth of the plant cell wall. Nature reviews molecular cell biology **6**: 850

Desnos T, Orbovic V, Bellini C, Kronenberger J, Caboche M, Traas J, Hofte H (1996) Procuste1 mutants identify two distinct genetic pathways controlling hypocotyl cell elongation, respectively in dark- and light-grown Arabidopsis seedlings. Development **122**: 683–693

Desprez T, Vernhettes S, Fagard M, Refrégier G, Desnos T, Aletti E, Py N, Pelletier S, Höfte H (2002) Resistance against herbicide isoxaben and cellulose deficiency caused by distinct mutations in same cellulose synthase isoform CESA6. Plant physiology **128**: 482–490

Du J, Kirui A, Huang S, Wang L, Barnes WJ, Kiemle SN, Zheng Y, Rui Y, Ruan M, Qi S, et al (2020) Mutations in the Pectin Methyltransferase QUASIMODO2 Influence Cellulose Biosynthesis and Wall Integrity in Arabidopsis. Plant Cell **32**: 3576

Engelsdorf T, Gigli-Bisceglia N, Veerabagu M, McKenna JF, Vaahtera L, Augstein F, Van der Does D, Zipfel C, Hamann T (2018) The plant cell wall integrity maintenance and immune signaling systems cooperate to control stress responses in Arabidopsis thaliana. Science Signaling 11:

Fagard M, Desnos T, Desprez T, Goubet F, Refregier G, Mouille G, McCann M, Rayon C, Vernhettes S, Höfte H (2000) PROCUSTE1 encodes a cellulose synthase required for normal cell elongation specifically in roots and dark-grown hypocotyls of Arabidopsis. The plant cell **12**: 2409–2423

Feng S, Martinez C, Gusmaroli G, Wang Y, Zhou J, Wang F, Chen L, Yu L, Iglesias-Pedraz JM, Kircher S, et al (2008) Coordinated regulation of Arabidopsis thaliana development by light and gibberellins. Nature **451**: 475–479

Feng W, Kita D, Peaucelle A, Cartwright HN, Doan V, Duan Q, Liu M-C, Maman J, Steinhorst L, Schmitz-Thom I (2018) The FERONIA receptor kinase maintains cell-wall integrity during salt stress through Ca2+ signaling. Current Biology **28**: 666-675. e5

Ferrari S, Galletti R, Vairo D, Cervone F, De Lorenzo G (2006) Antisense expression of the Arabidopsis thaliana AtPGIP1 gene reduces polygalacturonase-inhibiting protein accumulation and enhances susceptibility to Botrytis cinerea. Molecular Plant-Microbe Interactions **19**: 931–936

Floková K, Tarkowská D, Miersch O, Strnad M, Wasternack C, Novák O (2014) UHPLC–MS/MS based target profiling of stress-induced phytohormones. Phytochemistry **105**: 147–157

Franklin KA, Lee SH, Patel D, Kumar SV, Spartz AK, Gu C, Ye S, Yu P, Breen G, Cohen JD, et al (2011) PHYTOCHROME-INTERACTING FACTOR 4 (PIF4) regulates auxin biosynthesis at high temperature. Proceedings of the National Academy of Sciences **108**: 20231–20235

Freshour G, Bonin CP, Reiter W-D, Albersheim P, Darvill AG, Hahn MG (2003) Distribution of Fucose-Containing Xyloglucans in Cell Walls of the mur1 Mutant of Arabidopsis. Plant Physiology **131**: 1602

Griffiths J, Rizza A, Tang B, Frommer WB, Jones AM (2023) Gibberellin perception sensors 1 and 2 reveal cellular GA dynamics articulated by COP1 and GA20ox1 that are necessary but not sufficient to pattern hypocotyl cell elongation. BioRxiv 2023.11. 06.565859

Guzmán P, Ecker JR (1990) Exploiting the triple response of Arabidopsis to identify ethylene-related mutants. The Plant Cell **2**: 513–523

Hamann T, Bennett M, Mansfield J, Somerville C (2009) Identification of cell-wall stress as a hexose-dependent and osmosensitive regulator of plant responses. The Plant Journal **57**: 1015–1026

Hedden P, Phillips AL (2000) Gibberellin metabolism: new insights revealed by the genes. Trends in plant science **5**: 523–530

Heim DR, Skomp JR, Tschabold EE, Larrinua IM (1990) Isoxaben Inhibits the Synthesis of Acid Insoluble Cell Wall Materials In Arabidopsis thaliana. Plant Physiology **93**: 695–700

Heisler MG, Ohno C, Das P, Sieber P, Reddy GV, Long JA, Meyerowitz EM (2005) Patterns of Auxin Transport and Gene Expression during Primordium Development Revealed by Live Imaging of the Arabidopsis Inflorescence Meristem. Current Biology **15**: 1899–1911

Hématy K, Sado P-E, Van Tuinen A, Rochange S, Desnos T, Balzergue S, Pelletier S, Renou J-P, Höfte H (2007) A receptor-like kinase mediates the response of Arabidopsis cells to the inhibition of cellulose synthesis. Current Biology **17**: 922–931

Jonsson K, Hamant O, Bhalerao RP (2022) Plant cell walls as mechanical signaling hubs for morphogenesis. Current Biology **32**: R334–R340

Jonsson K, Lathe RS, Kierzkowski D, Routier-Kierzkowska A-L, Hamant O, Bhalerao RP (2021) Mechanochemical feedback mediates tissue bending required for seedling emergence. Current Biology **31**: 1154-1164. e3

Krupková E, Immerzeel P, Pauly M, Schmülling T (2007) The TUMOROUS SHOOT DEVELOPMENT2 gene of Arabidopsis encoding a putative methyltransferase is required for cell adhesion and co-ordinated plant development. The Plant Journal **50**: 735–750

Lehman A, Black R, Ecker JR (1996) HOOKLESS1, an Ethylene Response Gene, Is Required for Differential Cell Elongation in the Arabidopsis Hypocotyl. Cell **85**: 183–194

Li H, Johnson P, Stepanova A, Alonso JM, Ecker JR (2004) Convergence of signaling pathways in the control of differential cell growth in Arabidopsis. Developmental cell **7**: 193–204

Li K, Yu R, Fan L-M, Wei N, Chen H, Deng XW (2016) DELLA-mediated PIF degradation contributes to coordination of light and gibberellin signalling in Arabidopsis. Nat Commun **7**: 11868

Lin W, Tang W, Pan X, Huang A, Gao X, Anderson CT, Yang Z (2022) Arabidopsis pavement cell morphogenesis requires FERONIA binding to pectin for activation of ROP GTPase signaling. Current Biology **32**: 497-507.e4

Lorrai R, Ferrari S (2021) Host Cell Wall Damage during Pathogen Infection: Mechanisms of Perception and Role in Plant-Pathogen Interactions. Plants **10**: 399

de Lucas M, Davière J-M, Rodríguez-Falcón M, Pontin M, Iglesias-Pedraz JM, Lorrain S, Fankhauser C, Blázquez MA, Titarenko E, Prat S (2008) A molecular framework for light and gibberellin control of cell elongation. Nature **451**: 480–484

Merz D, Richter J, Gonneau M, Sanchez-Rodriguez C, Eder T, Sormani R, Martin M, Hématy K, Höfte H, Hauser M-T (2017) T-DNA alleles of the receptor kinase THESEUS1 with opposing effects on cell wall integrity signaling. Journal of Experimental Botany **68**: 4583–4593

Mielke S, Zimmer M, Meena MK, Dreos R, Stellmach H, Hause B, Voiniciuc C, Gasperini D (2021) Jasmonate biosynthesis arising from altered cell walls is prompted by turgor-driven mechanical compression. Science Advances **7**: eabf0356

Mølhøj M, Verma R, Reiter W-D (2004) The Biosynthesis of d-Galacturonate in Plants. Functional Cloning and Characterization of a Membrane-Anchored UDP-d-Glucuronate 4-Epimerase from Arabidopsis. Plant Physiology **135**: 1221–1230

Mouille G, Ralet M-C, Cavelier C, Eland C, Effroy D, Hématy K, McCartney L, Truong HN, Gaudon V, Thibault J-F (2007) Homogalacturonan synthesis in Arabidopsis thaliana requires a Golgi-localized protein with a putative methyltransferase domain. The Plant Journal **50**: 605–614

Nicol F, His I, Jauneau A, Vernhettes S, Canut H, Höfte H (1998) A plasma membrane-bound putative endo-1,4-β-d-glucanase is required for normal wall assembly and cell elongation in Arabidopsis. The EMBO Journal **17**: 5563–5576

Pfaffl MW (2001) A new mathematical model for relative quantification in real-time RT–PCR. Nucleic acids research **29**: e45–e45

Raggi S, Ferrarini A, Delledonne M, Dunand C, Ranocha P, De Lorenzo G, Cervone F, Ferrari S (2015) The Arabidopsis class III peroxidase AtPRX71 negatively regulates growth under physiological conditions and in response to cell wall damage. Plant physiology **169**: 2513–2525

Ray PM, Green PB, Cleland R (1972) Role of Turgor in Plant Cell Growth. Nature **239**: 163–164

Rayon C, Cabanes-Macheteau M, Loutelier-Bourhis C, Salliot-Maire I, Lemoine J, Reiter W-D, Lerouge P, Faye L (1999) Characterization of N-Glycans from Arabidopsis. Application to a Fucose-Deficient Mutant1. Plant Physiology **119**: 725–734

Reiter W-D, Chapple C, Somerville CR (1997) Mutants of Arabidopsis thaliana with altered cell wall polysaccharide composition. The Plant Journal **12**: 335–345

Reiter W-D, Chapple CC, Somerville CR (1993) Altered growth and cell walls in a fucose-deficient mutant of Arabidopsis. Science **261**: 1032–1035

Rizza A, Walia A, Lanquar V, Frommer WB, Jones AM (2017) In vivo gibberellin gradients visualized in rapidly elongating tissues. Nature Plants **3**: 803–813

Rouet M-A, Mathieu Y, Barbier-Brygoo H, Laurière C (2006) Characterization of active oxygen-producing proteins in response to hypo-osmolarity in tobacco and Arabidopsis cell suspensions: identification of a cell wall peroxidase. Journal of Experimental Botany **57**: 1323–1332

Rowe J, Grangé-Guermente M, Exposito-Rodriguez M, Wimalasekera R, Lenz MO, Shetty KN, Cutler SR, Jones AM (2023) Next-generation ABACUS biosensors reveal cellular ABA dynamics driving root growth at low aerial humidity. Nat Plants **9**: 1103–1115

Rowe JH, Rizza A, Jones AM (2022) Quantifying Phytohormones in Vivo with FRETFörster Resonance Energy Transfer (FRET)BiosensorsBiosensors and the FRETENATOR Analysis Toolset. *In* P Duque, D Szakonyi, eds, Environmental Responses in Plants: Methods and Protocols. Springer US, New York, NY, pp 239–253

Rui Y, Dinneny JR (2020) A wall with integrity: Surveillance and maintenance of the plant cell wall under stress. New Phytologist **225**: 1428–1439

Shen X, Li Y, Pan Y, Zhong S (2016) Activation of HLS1 by Mechanical Stress via Ethylene-Stabilized EIN3 Is Crucial for Seedling Soil Emergence. Frontiers in Plant Science 7:

Silk WK, Erickson RO (1978) Kinematics of Hypocotyl Curvature. American Journal of Botany **65**: 310–319

Sinclair SA, Larue C, Bonk L, Khan A, Castillo-Michel H, Stein RJ, Grolimund D, Begerow D, Neumann U, Haydon MJ, et al (2017) Etiolated Seedling Development Requires Repression of Photomorphogenesis by a Small Cell-Wall-Derived Dark Signal. Current Biology **27**: 3403-3418.e7

Široká J, Brunoni F, Pěnčík A, Mik V, Žukauskaitė A, Strnad M, Novák O, Floková K (2022) High-throughput interspecies profiling of acidic plant hormones using miniaturised sample processing. Plant Methods **18**: 122

Song S, Huang H, Gao H, Wang J, Wu D, Liu X, Yang S, Zhai Q, Li C, Qi T, et al (2014) Interaction between MYC2 and ETHYLENE INSENSITIVE3 Modulates Antagonism between Jasmonate and Ethylene Signaling in Arabidopsis. The Plant Cell **26**: 263–279

Sun T (2008) Gibberellin Metabolism, Perception and Signaling Pathways in Arabidopsis. Arabidopsis Book **6**: e0103

Vaahtera L, Schulz J, Hamann T (2019) Cell wall integrity maintenance during plant development and interaction with the environment. Nat Plants 5: 924–932.

Verger S, Long Y, Boudaoud A, Hamant O (2018) A tension-adhesion feedback loop in plant epidermis. Elife **7**: e34460

Wasternack C, Hause B (2013) Jasmonates: biosynthesis, perception, signal transduction and action in plant stress response, growth and development. An update to the 2007 review in Annals of Botany. Annals of Botany **111**: 1021–1058

Willis L, Refahi Y, Wightman R, Landrein B, Teles J, Huang KC, Meyerowitz EM, Jönsson H (2016) Cell size and growth regulation in the Arabidopsis thaliana apical stem cell niche. Proceedings of the National Academy of Sciences **113**: E8238–E8246

Wolf S, Hématy K, Höfte H (2012) Growth Control and Cell Wall Signaling in Plants. Annual Review of Plant Biology **63**: 381–407

Zhang B, Holmlund M, Lorrain S, Norberg M, Bakó L, Fankhauser C, Nilsson O (2017) BLADE-ON-PETIOLE proteins act in an E3 ubiquitin ligase complex to regulate PHYTOCHROME INTERACTING FACTOR 4 abundance. eLife **6**: e26759

Zhang X, Ji Y, Xue C, Ma H, Xi Y, Huang P, Wang H, An F, Li B, Wang Y (2018) Integrated regulation of apical hook development by transcriptional coupling of EIN3/EIL1 and PIFs in Arabidopsis. The Plant Cell **30**: 1971–1988

Zhang X, Zhu Z, An F, Hao D, Li P, Song J, Yi C, Guo H (2014) Jasmonate-Activated MYC2 Represses ETHYLENE INSENSITIVE3 Activity to Antagonize Ethylene-Promoted Apical Hook Formation in Arabidopsis. The Plant Cell **26**: 1105–1117

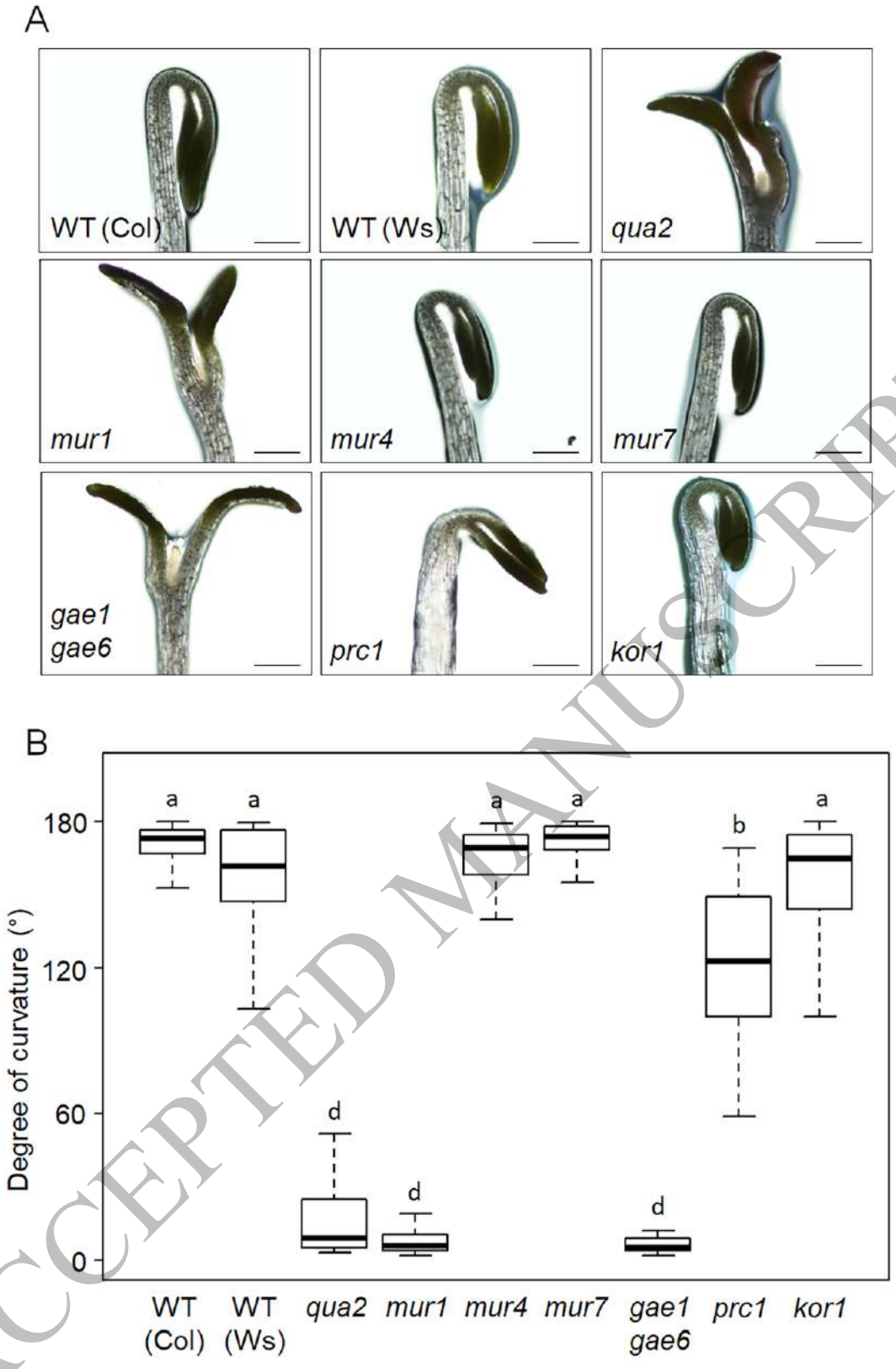

Figure 1. Apical hook formation in Arabidopsis cell wall mutants. (**A**) Representative pictures of wild-type (WT) Columbia-0 (Col), WT Wassilewskija (Ws), *qua2*, *mur1*, *mur4*, *mur7*, *gae1gae6*, *prc1* (in Col-0 background) and *kor1* (in Ws background) three days after germination. Scale bars in all panels, 0.5 mm. (**B**) Quantification of apical hook angles of seedlings grown as in (**A**). Box plots indicate the 1st and 3rd quartiles split by median; whiskers show range (n≥20). Letters indicate statistically significant differences ($p<0.05$) according to one-way ANOVA followed by post-hoc Tukey's HSD.

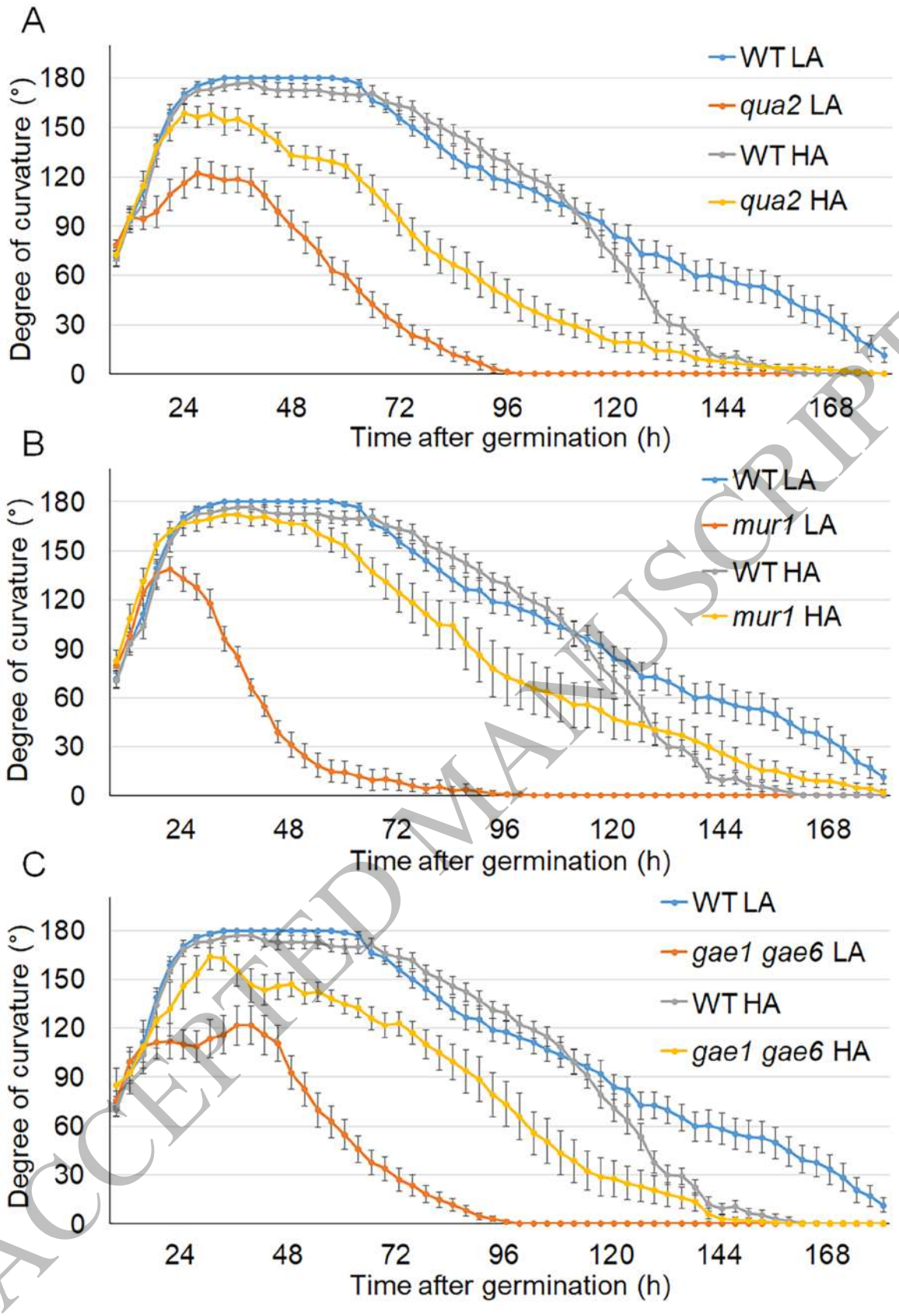

Figure 2. Kinematic analysis of apical hook formation in pectin mutants grown on low and high agar. Wild-type (WT, blue and grey lines) and *qua2* (**A**), *mur1* (**B**) or *gae1gae6* (**C**) mutant (orange and yellow lines) seedlings were grown in the dark on medium containing either 0.8% (w/v) (LA, blue and orange lines) or 2.5% (w/v) agar (HA, gray and yellow lines). The hook angle was measured at the indicated times. Error bars represent mean angle ± SE (n≥15).

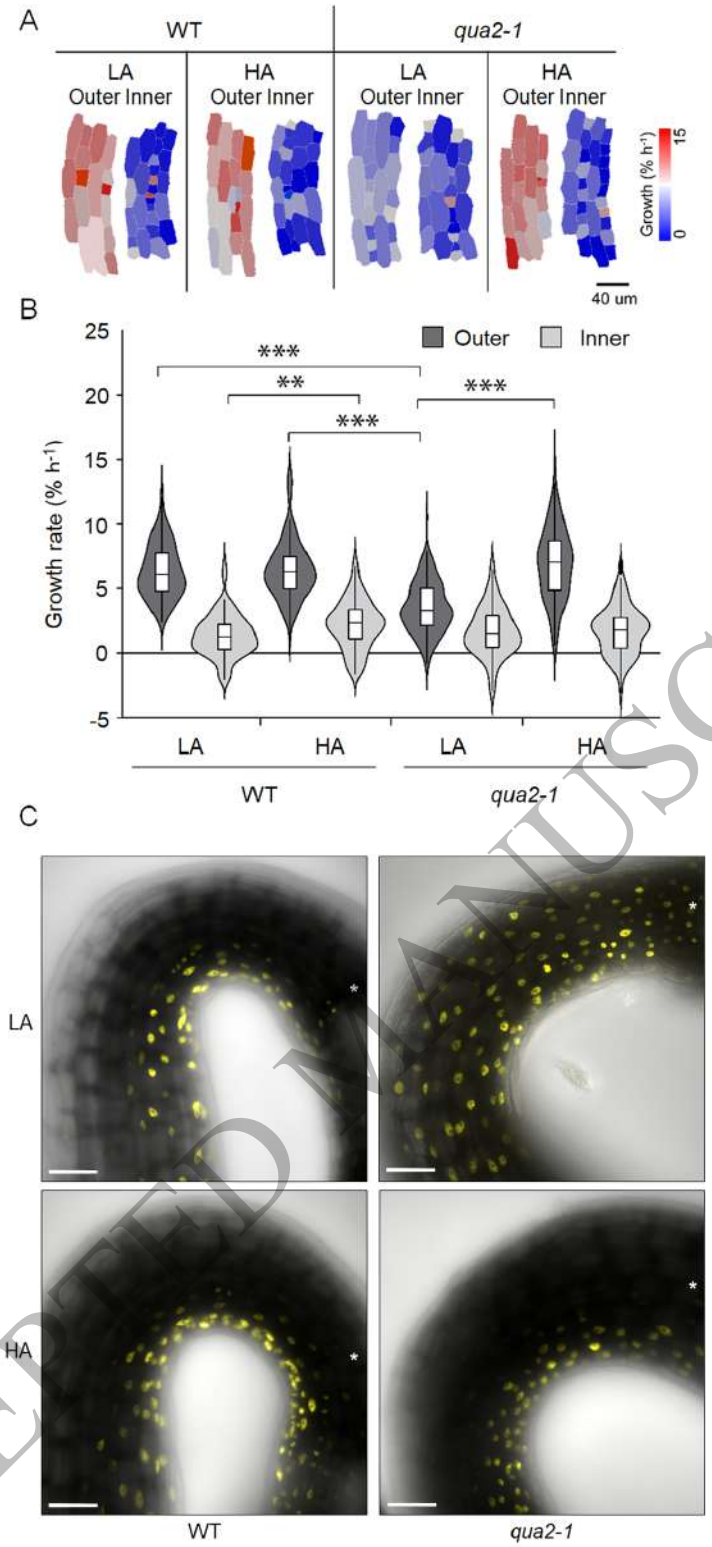

Figure 3. Effects of agar concentration on cell elongation and auxin response during apical hook formation in *qua2* seedlings. (**A**) Heatmaps of the growth rate of individual cells in the apical portion of the hypocotyl upon a three-hour time lapse in wild-type (WT) and *qua2* seedlings grown in the dark on medium containing 0.8% (LA) or 2.5% (HA) (w/v) agar. (**B**) Quantification of the growth rate of individual cells in the outer (dark grey) and inner (light grey) side of the hypocotyl of seedlings grown as in (**A**). Data are average of three independent biological replicates ± SD. In violin plots, the box limits represent the 1st and 3rd quartiles split by median, whiskers show range. For each experiment, 15 cells from both the inner and outer sides of the hook were measured from each of 9 individual seedlings. Asterisks indicate statistical significance by Student's t-test (**, $p<0.01$; ***, $p<0.001$). (**C**) Representative confocal laser scanning microscopy images of WT and *qua2* seedlings expressing the DR5::Venus-NLS and grown in the dark on LA or HA. White asterisks in (**C**) mark position of SAM. Scale bars in all panels, 50 µm.

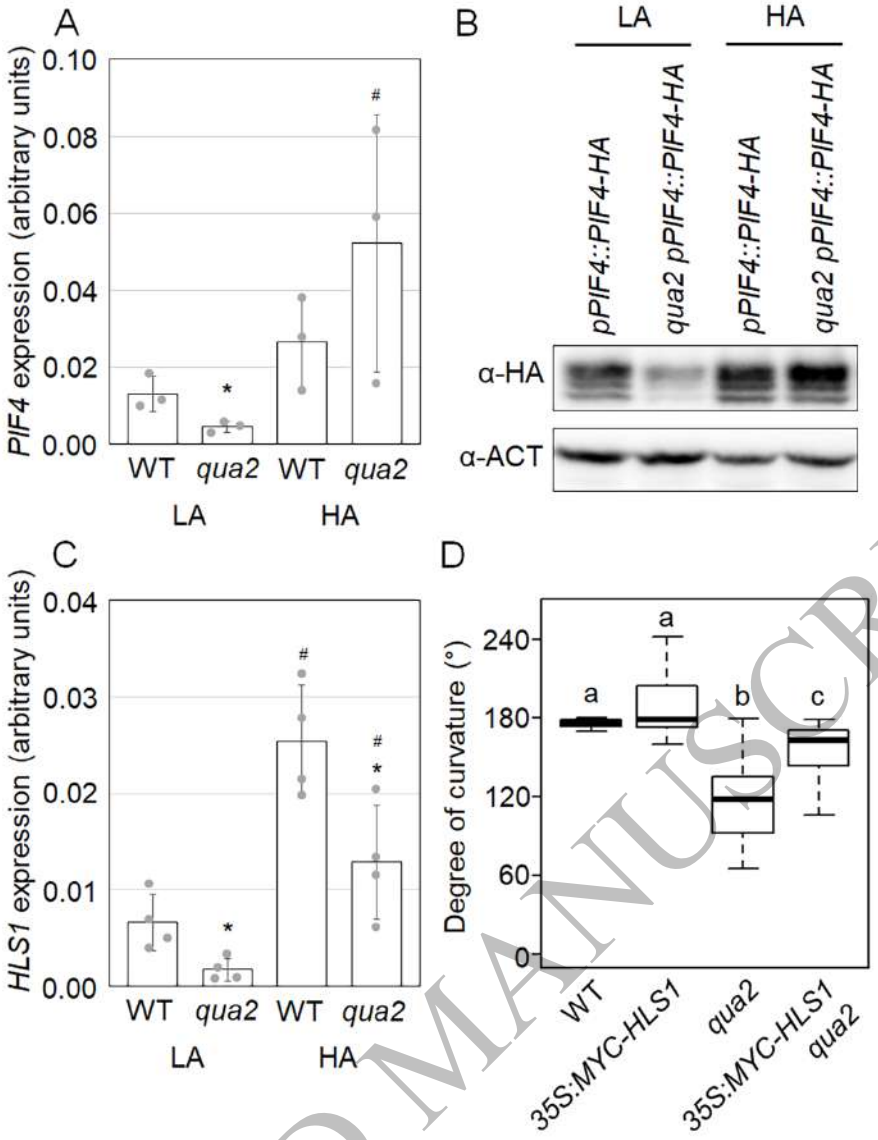

Figure 4. *HLS1* and *PIF4* expression in *qua2* mutant. Total RNA was extracted from wild-type (WT) and *qua2* seedlings two days after germination grown in the dark on medium containing 0.8% (LA) or 2.5% (HA) agar (w/v). (**A**) Expression of *PIF4* was analysed by RT-qPCR, using *UBQ5* as a reference. (**B**) Transgenic lines expressing PIF4-HA under the control of its native promoter (ProPIF4:PIF4-3×HA) in *pif4*-101 or *qua2-1* background were grown on LA or HA medium. PIF4-HA levels were detected by immunoblot analysis with an antibody against HA; an antibody against actin (ACT) was used as a loading control. (**C**) Expression of *HLS1* was analysed by RT-qPCR, using *UBQ5* as a reference. Bars (in **A** and **C**) indicate mean of at least three independent biological replicates ± SD. Asterisks indicate statistically significant differences with WT according to Student's t-test (*, $p<0.05$), number signs indicate statistically significant differences with LA between same genotype according to Student's t-test (#, $p<0.05$). (**D**) Quantification of apical hook angles of wild-type (WT), 35S:Myc-HLS1/*hls1-1*, *qua2*, and *qua2* 35S:Myc-HLS1/*hls1-1* seedlings two days after germination grown in the dark. Box plots in (**D**) indicate the 1st and 3rd quartiles split by median; whiskers show range ($n\geq20$). Letters indicate statistically significant differences ($p<0.05$) according to one-way ANOVA followed by post-hoc Tukey's HSD.

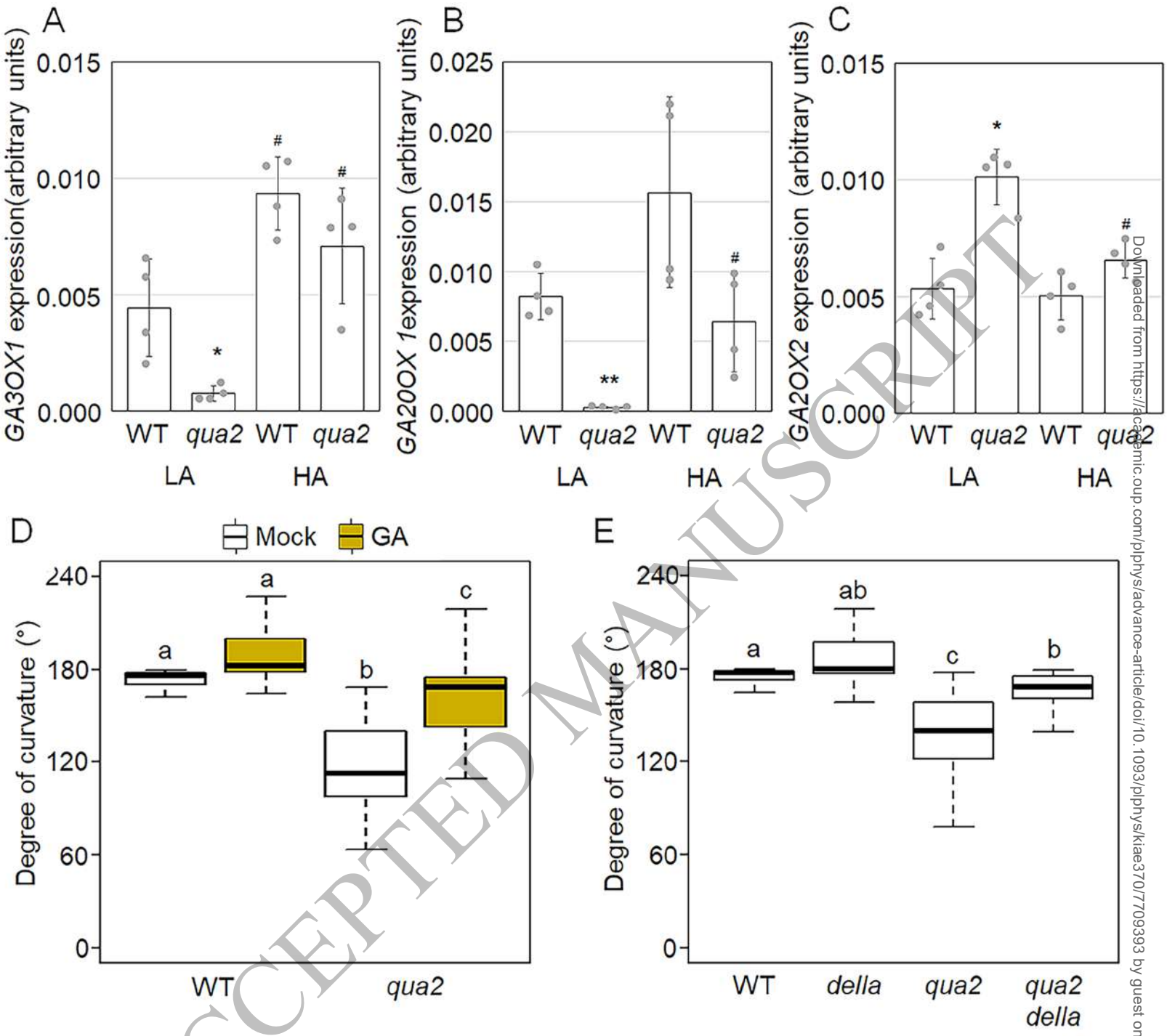

Figure 5. Defects in the expression of GA biosynthetic genes in *qua2* mutant. Expression of *GA3ox1* (**A**), *GA20ox1* (**B**) and *GA2ox2* (**C**) in WT and *qua2* seedlings grown in LA and HA. Transcript levels were determined by RT-qPCR using *UBQ5* as a reference. Bars indicate mean of at least three independent biological replicates ± SD. Asterisks indicate statistically significant differences with WT according to Student's t-test (*, $p<0.05$; **, $p<0.01$), number signs indicate statistically significant differences with LA between same genotype according to Student's t-test (#, $p<0.05$). (**D**) Apical hook angles of WT and *qua2* seedlings two days after germination grown in the dark on medium supplemented with ethanol (mock, white boxes) or 50 µM GA_4 (GA, yellow boxes). (**E**) Apical hook angles of wild-type Ler (WT), *della*, *qua2* and *qua2 della* sixtuple mutant seedlings two days after germination grown in the dark. Box plots in (**D**-**E**) indicate the 1st and 3rd quartiles split by median; whiskers show range (n≥20). Letters indicate statistically significant differences, according to two-way ANOVA followed by post-hoc Tukey's HSD ($p<0.05$).

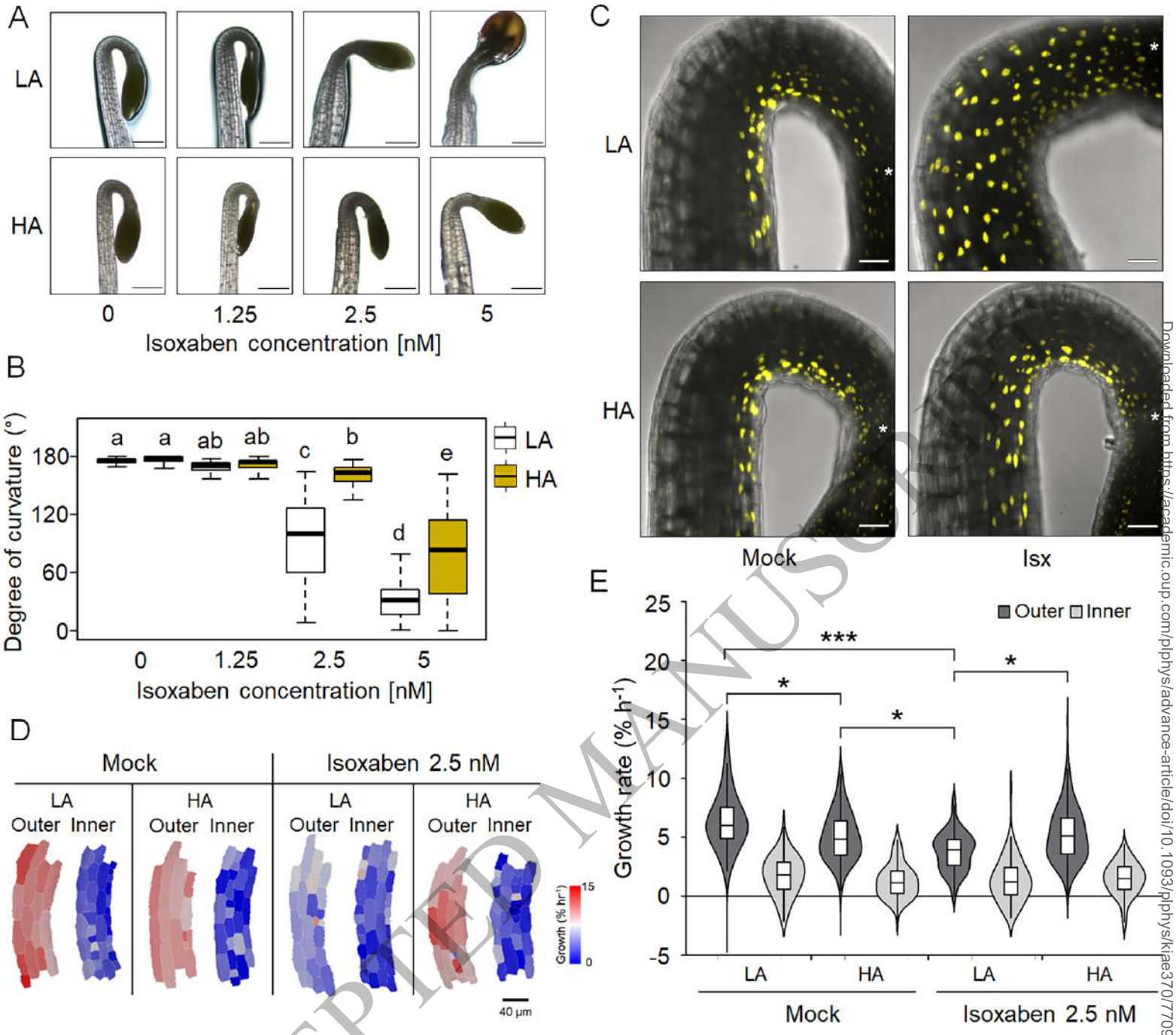

Figure 6. Isoxaben inhibits apical hook formation in a turgor-dependent manner. (**A**) Representative pictures of wild-type (WT) seedlings two days after germination grown in the dark on medium 0.8% (LA) or 2.5% (HA) agar (w/v) and supplemented with isoxaben (isx) at the indicated doses. Scale bars in all panels, 0.5 mm. (**B**) Quantification of apical hook angles of WT seedlings grown as in (**A**). Box plots in (**B**) indicate the 1st and 3rd quartiles split by median; whiskers show range (n≥20). Letters indicate statistically significant differences, according to two-way ANOVA followed by post-hoc Tukey's HSD ($p<0.05$). (**C**) Representative confocal laser scanning microscopy images of WT seedlings expressing the DR5::Venus-NLS grown in the dark with 2.5 nM isx in the dark on LA or HA. White asterisks in (**C**) mark the position of SAM. Scale bars in all panels, 50 µm. (**D**) Heatmaps of the growth rate of individual cells in the apical portion of the hypocotyl upon a three-hour time lapse in wild-type (WT) grown in the dark on medium containing 0.8% (LA) or 2.5% (HA) (w/v) agar supplemented with 2.5 nM isx. (**E**) Quantification of the growth rate of individual cells in the outer (dark grey) and inner (light grey) side of the hypocotyl of seedlings grown as in (**D**). Data are average of three independent biological replicates ± SD. In violin plots, the box limits represent the 1st and 3rd quartiles split by median, whiskers show range. For each experiment, 15 cells from both the inner and outer sides of the hook were measured from each of 9 individual seedlings. Asterisks indicate statistical significance by Student's t-test (*, $p<0.05$; ***, $p<0.001$).

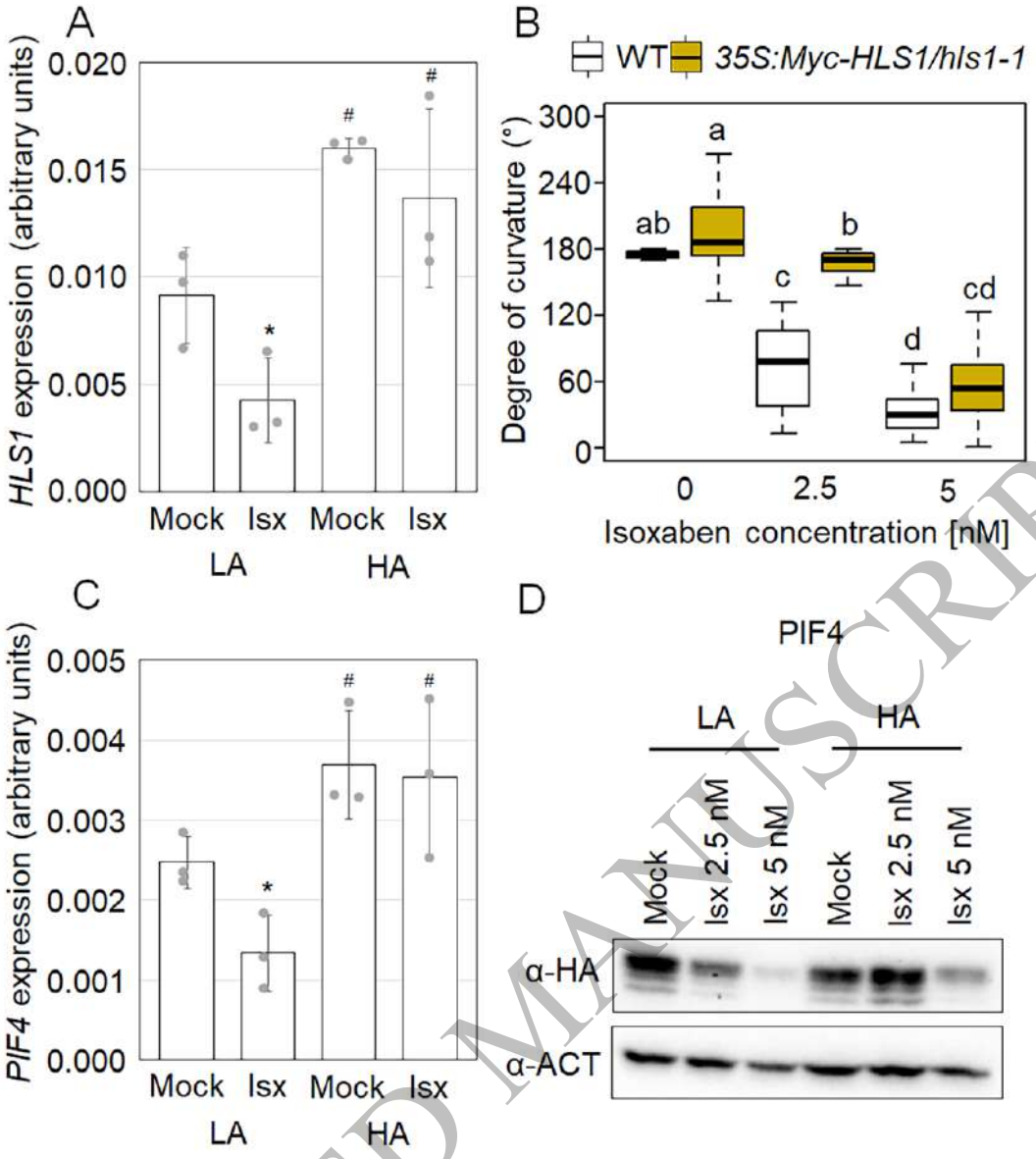

Figure 7. Isoxaben inhibits *PIF4* and *HLS1* expression in a turgor-dependent manner. (**A**) Expression of *HLS1* in WT seedlings two days after germination grown in the dark with 2.5 nM isx in LA and HA. Transcript levels were determined by RT-qPCR using *UBQ5* as a reference. (**B**) Quantification of apical hook angles of wild-type (WT) and 35S:Myc-HLS1/*hls1-1* seedlings two days after germination grown in the dark in the presence of the indicated concentrations of isx (WT, white boxes; 35S:Myc-HLS1/*hls1-1*, yellow boxes). (**C**) Expression of *PIF4* in WT seedlings two days after germination grown in the dark with 2.5 nM isx in LA and HA. Transcript levels were determined by RT-qPCR using *UBQ5* as a reference. (**D**) Transgenic lines expressing PIF4-HA under the control of its native promoter (ProPIF4:PIF4-3×HA) in *pif4*-101 background were grown on LA or HA medium supplemented with the indicated concentrations of isx. PIF4-HA levels were detected by immunoblot analysis with an antibody against HA; an antibody against actin (ACT) was used as a loading control. Bars in (**A** and **C**) indicate mean of at least three independent biological replicates ± SD. Asterisks indicate statistically significant differences between mock- and isx-treated seedlings according to Student's t-test (*, $p<0.05$); number signs indicate statistically significant differences between similarly treated seedlings grown on LA or HA according to Student's t-test (#, $p<0.05$). Letters in (**B**) indicate statistically significant differences according to two-way ANOVA followed by post-hoc Tukey's HSD ($p<0.05$). Box plots indicate the 1st and 3rd quartiles split by median; whiskers show range ($n\geq20$).

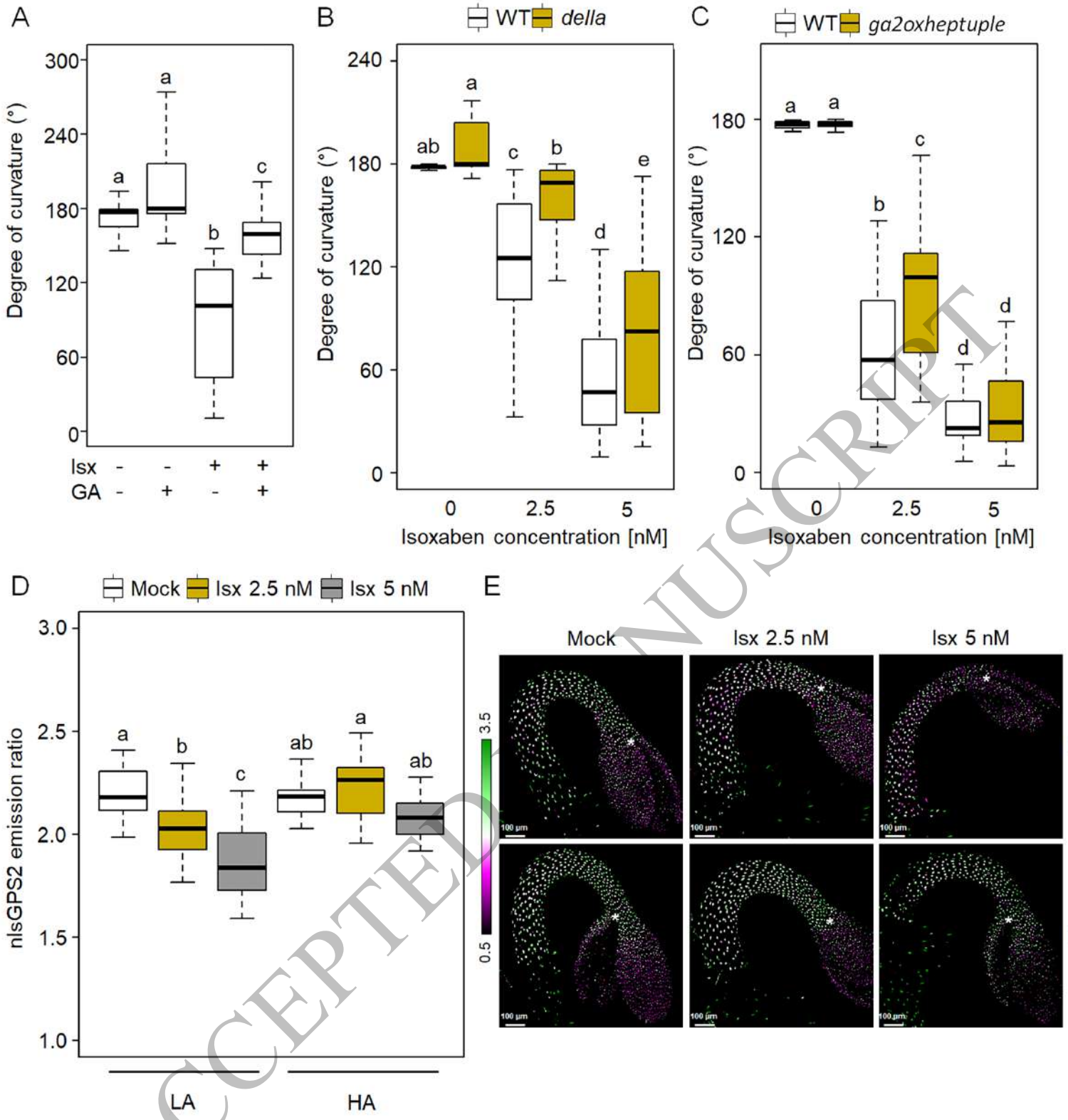

Figure 8. Isoxaben inhibits GA accumulation and signalling in a turgor-dependent manner. (**A**) Apical hook angles of WT seedlings two days after germination grown in the dark and treated with DMSO or 2.5 nM isoxaben (isx) in the presence or absence of 50 µM GAs. (**B**) Apical hook angles of wild-type Ler (WT, white boxes) and *della* (yellow boxes) seedlings two days after germination grown in the dark in the presence of isx at the indicated doses. (**C**) Apical hook angles of wild-type Col-0 (WT, white boxes) and *GA2oxheptuple* (yellow boxes) seedlings two days after germination grown in the dark in the presence of isx at the indicated doses. (**D**) nlsGPS2 nuclear emission ratios from n≥8 hypocotyls of seedlings one day after germination grown in the dark in the presence of the indicated amount of isx on medium containing 0.8% (LA) or 2.5% (HA) agar (w/v). (**E**) Representative images of nlsGPS2 emission ratios of the hypocotyls of seedlings grown as in (**D**). Letters in **(A-D)** indicate statistically significant differences according to two-way ANOVA followed by post-hoc Tukey's HSD ($p<0.05$). Box plots indicate the 1st and 3rd quartiles split by median; whiskers show range (n≥20) in (**A-C**) (n≥12) in (**D**). White asterisks in (**E**) mark position of SAM, scale bars in all panels, 100 µm.

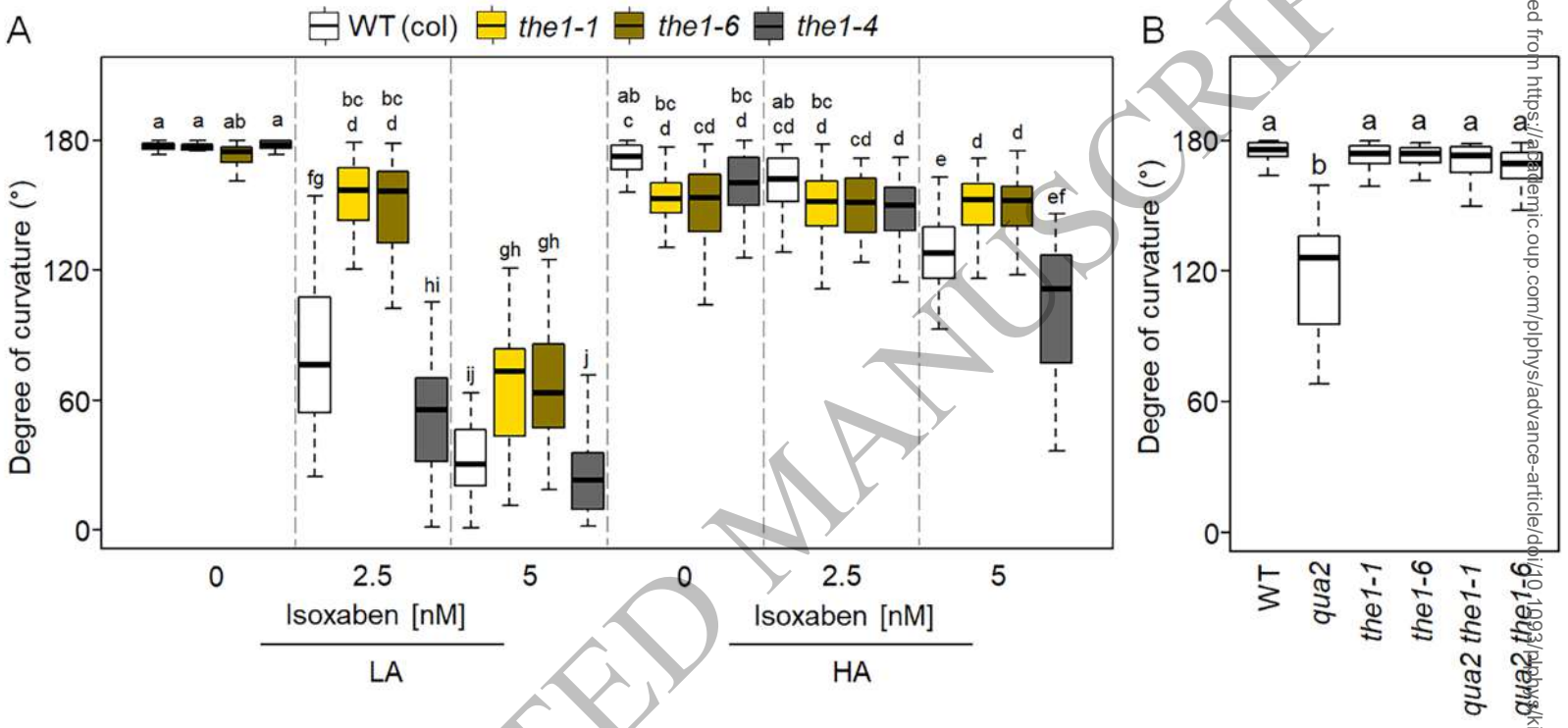

Figure 9. Apical hook inhibitions by isoxaben supplementation or *qua2* mutation is dependent on THE1. (**A**) Quantification of apical hook angles of WT (Col-0), *the1-1*, *the1-6* and *the1-4* seedlings two days after germination grown in the dark on medium 0.8% (LA) or 2.5% (HA) agar (w/v) and supplemented with isoxaben (isx) at the indicated doses. (**B**) Quantification of apical hook angles of WT, *qua2*, *the1-1*, *the1-6*, *qua2 the1-1* and *qua2 the1-6* seedlings two days after germination grown in the dark. Letters indicate statistically significant differences according to two-way ANOVA followed by post-hoc Tukey's HSD ($p<0.05$). Box plots indicate the 1st and 3rd quartiles split by median; whiskers show range ($n\geq20$).

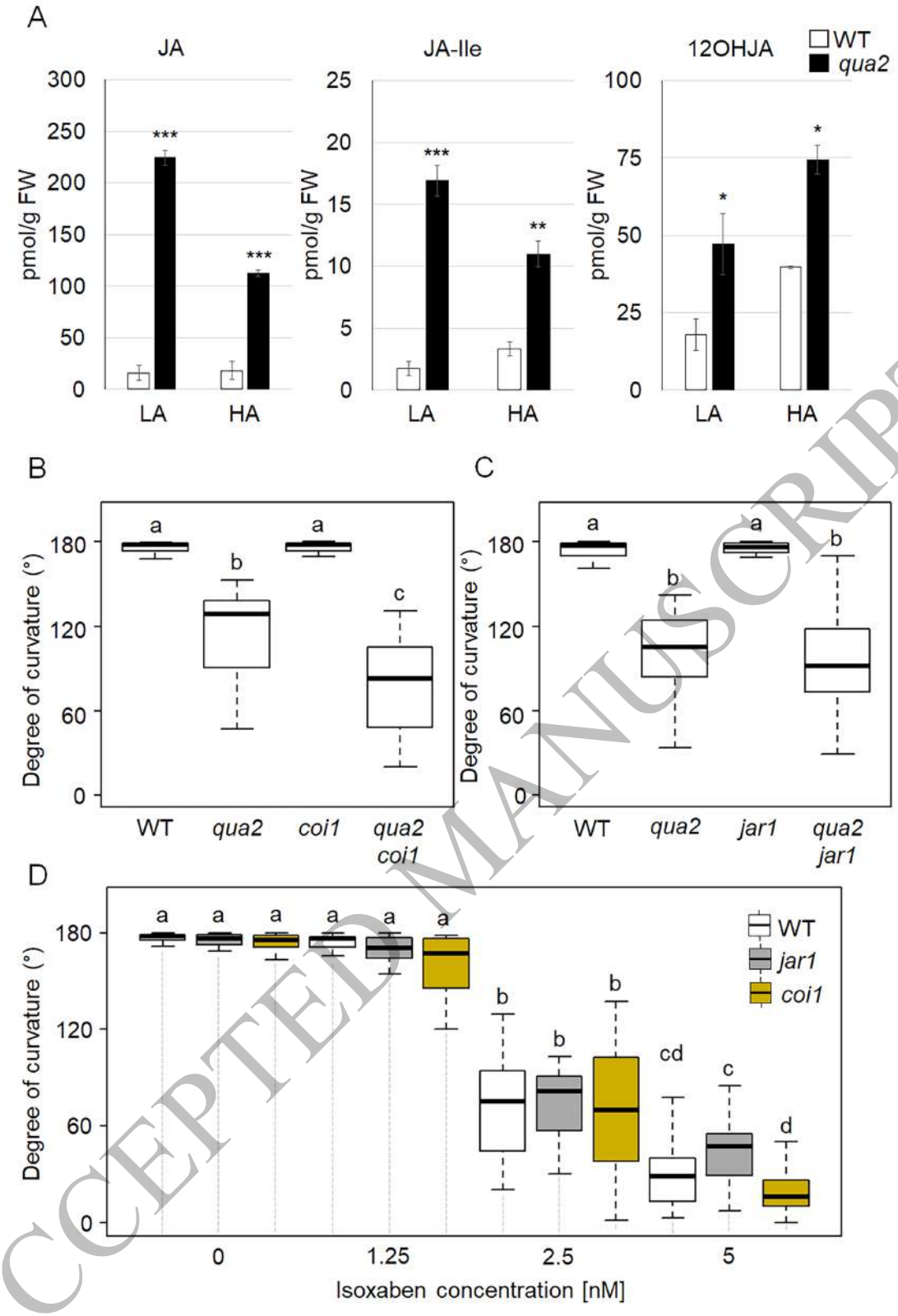

Figure 10. Inhibition of apical hook formation in response to altered cell wall integrity is independent of jasmonate signalling. (**A**) Levels of JA, JA-Ile, Σ 11-/12-OHJA in wild-type (WT, white bars) and *qua2* (black bars) seedlings two days after germination grown in the dark on medium containing 0.8% (LA) or 2.5% (HA) agar (w/v). Bars represent means of three independent biological replicates ± SD. Asterisks indicate significant differences relative to WT, according to Student's t-test (*p≤0.05, **p≤0.01, ***p≤0.001). (**B-C**) Apical hook angles of WT, *qua2*, *coi1* and *qua2 coi1* (**B**), or *jar1* and *qua2 jar1* (**C**) grown as in (**A**). (**D**) Quantification of apical hook angles of wild type (WT Columbia), *jar1* and *coi1* seedlings two days after germination grown in the dark in the presence of isoxaben (isx) at the indicated doses (WT, white boxes; *jar1*, grey boxes; *coi1* yellow boxes). Box plots in (**B-D**) indicate the 1st and 3rd quartiles split by median, and whiskers show range (n≥20). Letters indicate statistically significant differences ($p<0.05$) according to two-way ANOVA followed by post-hoc Tukey's HSD.

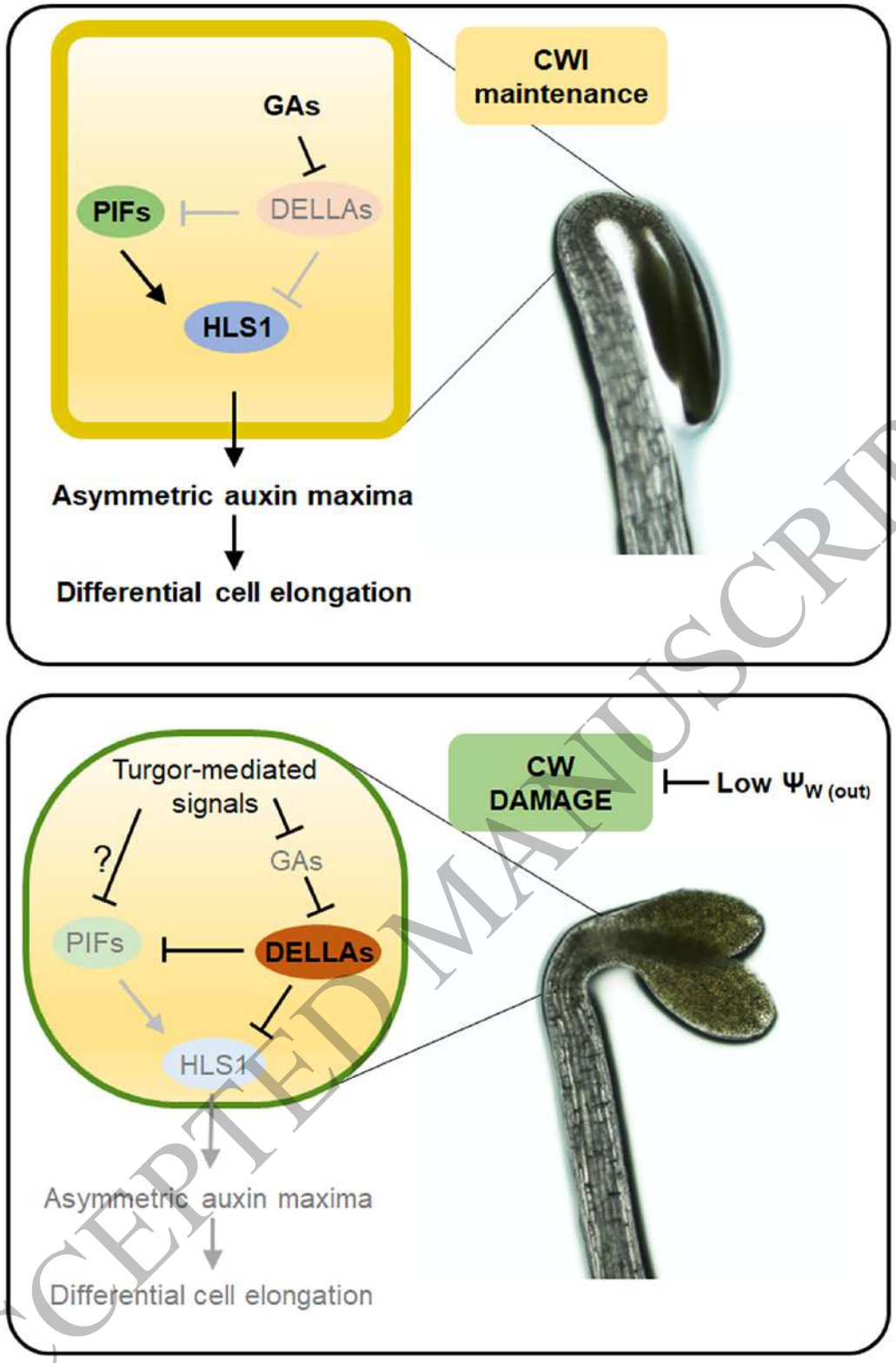

Figure 11. Proposed model of the effects of loss of cell wall integrity on apical hook formation. Perturbation of cell wall integrity (CWI), either caused by mutations in pectin composition or by isoxaben, activates turgor-dependent responses that repress accumulation of active gibberellins (GAs), leading to stabilization of DELLA proteins and reduction of PIF4 and possibly other PIFs protein levels. Increased DELLAs and reduced PIFs result in impaired *HLS1* expression, impairing proper formation of auxin response maxima and differential cell elongation, and ultimately inhibiting apical hook development. The arrows indicate positive regulation, and blunt-ended bars indicate inhibition. Question mark indicates unidentified signalling elements. Elements in grey indicate reduction of levels or reduced downstream responses. Ψ_w, water potential; PIFs, PHYTOCHROME-INTERACTING FACTORs; HLS1, HOOKLESS 1; DELLAs, DELLA proteins; GAs, gibberellins; CW, cell wall; CWI, cell wall integrity.

Parsed Citations

Abbas M, Alabadí D, Blázquez MA (2013) Differential growth at the apical hook: all roads lead to auxin. Frontiers in Plant Science 4:

Google Scholar: Author Only Title Only Author and Title

An F, Zhang X, Zhu Z, Ji Y, He W, Jiang Z, Li M, Guo H (2012) Coordinated regulation of apical hook development by gibberellins and ethylene in etiolated Arabidopsis seedlings. Cell Res 22: 915–927

Google Scholar: Author Only Title Only Author and Title

Aryal B, Jonsson K, Baral A, Sancho-Andres G, Routier-Kierzkowska A-L, Kierzkowski D, Bhalerao RP (2020) Interplay between cell wall and auxin mediates the control of differential cell elongation during apical hook development. Current Biology 30: 1733-1739. e3

Google Scholar: Author Only Title Only Author and Title

Bacete L, Hamann T (2020) The Role of Mechanoperception in Plant Cell Wall Integrity Maintenance. Plants 9: 574

Google Scholar: Author Only Title Only Author and Title

Bacete L, Schulz J, Engelsdorf T, Bartosova Z, Vaahtera L, Yan G, Gerhold JM, Tichá T, Øvstebø C, Gigli-Bisceglia N, et al (2022) THESEUS1 modulates cell wall stiffness and abscisic acid production in Arabidopsis thaliana. Proc Natl Acad Sci U S A 119: e2119258119

Google Scholar: Author Only Title Only Author and Title

Baral A, Aryal B, Jonsson K, Morris E, Demes E, Takatani S, Verger S, Xu T, Bennett M, Hamant O, et al (2021) External Mechanical Cues Reveal a Katanin-Independent Mechanism behind Auxin-Mediated Tissue Bending in Plants. Developmental Cell 56: 67-80.e3

Google Scholar: Author Only Title Only Author and Title

Barbier de Reuille P, Routier-Kierzkowska A-L, Kierzkowski D, Bassel GW, Schüpbach T, Tauriello G, Bajpai N, Strauss S, Weber A, Kiss A, et al (2015) MorphoGraphX: A platform for quantifying morphogenesis in 4D. eLife 4: e05864

Google Scholar: Author Only Title Only Author and Title

Bethke G, Thao A, Xiong G, Li B, Soltis NE, Hatsugai N, Hillmer RA, Katagiri F, Kliebenstein DJ, Pauly M (2016) Pectin biosynthesis is critical for cell wall integrity and immunity in Arabidopsis thaliana. The Plant Cell 28: 537–556

Google Scholar: Author Only Title Only Author and Title

Bonin CP, Potter I, Vanzin GF, Reiter W-D (1997) The MUR1 gene of Arabidopsis thaliana encodes an isoform of GDP-d-mannose-4,6-dehydratase, catalyzing the first step in the de novo synthesis of GDP-l-fucose. Proceedings of the National Academy of Sciences 94: 2085–2090

Google Scholar: Author Only Title Only Author and Title

Bouton S, Leboeuf E, Mouille G, Leydecker M-T, Talbotec J, Granier F, Lahaye M, Höfte H, Truong H-N (2002) QUASIMODO1 encodes a putative membrane-bound glycosyltransferase required for normal pectin synthesis and cell adhesion in Arabidopsis. The Plant Cell 14: 2577–2590

Google Scholar: Author Only Title Only Author and Title

Burget EG, Verma R, Molhoj M, Reiter WD (2003) Molecular cloning and characterization of a golgi-localized UDP-d-xylose 4-epimerase encoded by the MUR4 gene of Arabidopsis. Plant Cell 15: 31

Google Scholar: Author Only Title Only Author and Title

Cosgrove DJ (2005) Growth of the plant cell wall. Nature reviews molecular cell biology 6: 850

Google Scholar: Author Only Title Only Author and Title

Desnos T, Orbovic V, Bellini C, Kronenberger J, Caboche M, Traas J, Hofte H (1996) Procuste1 mutants identify two distinct genetic pathways controlling hypocotyl cell elongation, respectively in dark-and light-grown Arabidopsis seedlings. Development 122: 683–693

Google Scholar: Author Only Title Only Author and Title

Desprez T, Vernhettes S, Fagard M, Refrégier G, Desnos T, Aletti E, Py N, Pelletier S, Höfte H (2002) Resistance against herbicide isoxaben and cellulose deficiency caused by distinct mutations in same cellulose synthase isoform CESA6. Plant physiology 128: 482–490

Google Scholar: Author Only Title Only Author and Title

Du J, Kirui A, Huang S, Wang L, Barnes WJ, Kiemle SN, Zheng Y, Rui Y, Ruan M, Qi S, et al (2020) Mutations in the Pectin Methyltransferase QUASIMODO2 Influence Cellulose Biosynthesis and Wall Integrity in Arabidopsis. Plant Cell 32: 3576

Google Scholar: Author Only Title Only Author and Title

Engelsdorf T, Gigli-Bisceglia N, Veerabagu M, McKenna JF, Vaahtera L, Augstein F, Van der Does D, Zipfel C, Hamann T (2018) The plant cell wall integrity maintenance and immune signaling systems cooperate to control stress responses in Arabidopsis thaliana. Science Signaling 11:

Google Scholar: Author Only Title Only Author and Title

Fagard M, Desnos T, Desprez T, Goubet F, Refregier G, Mouille G, McCann M, Rayon C, Vernhettes S, Höfte H (2000) PROCUSTE1 encodes a cellulose synthase required for normal cell elongation specifically in roots and dark-grown hypocotyls of Arabidopsis. The plant cell 12: 2409–2423
Google Scholar: Author Only Title Only Author and Title

Feng S, Martinez C, Gusmaroli G, Wang Y, Zhou J, Wang F, Chen L, Yu L, Iglesias-Pedraz JM, Kircher S, et al (2008) Coordinated regulation of Arabidopsis thaliana development by light and gibberellins. Nature 451: 475–479
Google Scholar: Author Only Title Only Author and Title

Feng W, Kita D, Peaucelle A, Cartwright HN, Doan V, Duan Q, Liu M-C, Maman J, Steinhorst L, Schmitz-Thom I (2018) The FERONIA receptor kinase maintains cell-wall integrity during salt stress through Ca2+ signaling. Current Biology 28: 666-675. e5
Google Scholar: Author Only Title Only Author and Title

Ferrari S, Galletti R, Vairo D, Cervone F, De Lorenzo G (2006) Antisense expression of the Arabidopsis thaliana AtPGIP1 gene reduces polygalacturonase-inhibiting protein accumulation and enhances susceptibility to Botrytis cinerea. Molecular Plant-Microbe Interactions 19: 931–936
Google Scholar: Author Only Title Only Author and Title

Floková K, Tarkowská D, Miersch O, Strnad M, Wasternack C, Novák O (2014) UHPLC–MS/MS based target profiling of stress-induced phytohormones. Phytochemistry 105: 147–157
Google Scholar: Author Only Title Only Author and Title

Franklin KA, Lee SH, Patel D, Kumar SV, Spartz AK, Gu C, Ye S, Yu P, Breen G, Cohen JD, et al (2011) PHYTOCHROME-INTERACTING FACTOR 4 (PIF4) regulates auxin biosynthesis at high temperature. Proceedings of the National Academy of Sciences 108: 20231–20235
Google Scholar: Author Only Title Only Author and Title

Freshour G, Bonin CP, Reiter W-D, Albersheim P, Darvill AG, Hahn MG (2003) Distribution of Fucose-Containing Xyloglucans in Cell Walls of the mur1 Mutant of Arabidopsis. Plant Physiology 131: 1602
Google Scholar: Author Only Title Only Author and Title

Griffiths J, Rizza A, Tang B, Frommer WB, Jones AM (2023) Gibberellin perception sensors 1 and 2 reveal cellular GA dynamics articulated by COP1 and GA20ox1 that are necessary but not sufficient to pattern hypocotyl cell elongation. BioRxiv 2023.11. 06.565859
Google Scholar: Author Only Title Only Author and Title

Guzmán P, Ecker JR (1990) Exploiting the triple response of Arabidopsis to identify ethylene-related mutants. The Plant Cell 2: 513–523
Google Scholar: Author Only Title Only Author and Title

Hamann T, Bennett M, Mansfield J, Somerville C (2009) Identification of cell-wall stress as a hexose-dependent and osmosensitive regulator of plant responses. The Plant Journal 57: 1015–1026
Google Scholar: Author Only Title Only Author and Title

Hedden P, Phillips AL (2000) Gibberellin metabolism: new insights revealed by the genes. Trends in plant science 5: 523–530
Google Scholar: Author Only Title Only Author and Title

Heim DR, Skomp JR, Tschabold EE, Larrinua IM (1990) Isoxaben Inhibits the Synthesis of Acid Insoluble Cell Wall Materials In Arabidopsis thaliana. Plant Physiology 93: 695–700
Google Scholar: Author Only Title Only Author and Title

Heisler MG, Ohno C, Das P, Sieber P, Reddy GV, Long JA, Meyerowitz EM (2005) Patterns of Auxin Transport and Gene Expression during Primordium Development Revealed by Live Imaging of the Arabidopsis Inflorescence Meristem. Current Biology 15: 1899–1911
Google Scholar: Author Only Title Only Author and Title

Hématy K, Sado P-E, Van Tuinen A, Rochange S, Desnos T, Balzergue S, Pelletier S, Renou J-P, Höfte H (2007) A receptor-like kinase mediates the response of Arabidopsis cells to the inhibition of cellulose synthesis. Current Biology 17: 922–931
Google Scholar: Author Only Title Only Author and Title

Jonsson K, Hamant O, Bhalerao RP (2022) Plant cell walls as mechanical signaling hubs for morphogenesis. Current Biology 32: R334–R340
Google Scholar: Author Only Title Only Author and Title

Jonsson K, Lathe RS, Kierzkowski D, Routier-Kierzkowska A-L, Hamant O, Bhalerao RP (2021) Mechanochemical feedback mediates tissue bending required for seedling emergence. Current Biology 31: 1154-1164. e3
Google Scholar: Author Only Title Only Author and Title

Krupková E, Immerzeel P, Pauly M, Schmülling T (2007) The TUMOROUS SHOOT DEVELOPMENT2 gene of Arabidopsis

encoding a putative methyltransferase is required for cell adhesion and co-ordinated plant development. The Plant Journal 50: 735–750
Google Scholar: Author Only Title Only Author and Title

Lehman A, Black R, Ecker JR (1996) HOOKLESS1, an Ethylene Response Gene, Is Required for Differential Cell Elongation in the Arabidopsis Hypocotyl. Cell 85: 183–194
Google Scholar: Author Only Title Only Author and Title

Li H, Johnson P, Stepanova A, Alonso JM, Ecker JR (2004) Convergence of signaling pathways in the control of differential cell growth in Arabidopsis. Developmental cell 7: 193–204
Google Scholar: Author Only Title Only Author and Title

Li K, Yu R, Fan L-M, Wei N, Chen H, Deng XW (2016) DELLA-mediated PIF degradation contributes to coordination of light and gibberellin signalling in Arabidopsis. Nat Commun 7: 11868
Google Scholar: Author Only Title Only Author and Title

Lin W, Tang W, Pan X, Huang A, Gao X, Anderson CT, Yang Z (2022) Arabidopsis pavement cell morphogenesis requires FERONIA binding to pectin for activation of ROP GTPase signaling. Current Biology 32: 497-507.e4
Google Scholar: Author Only Title Only Author and Title

Lorrai R, Ferrari S (2021) Host Cell Wall Damage during Pathogen Infection: Mechanisms of Perception and Role in Plant-Pathogen Interactions. Plants 10: 399
Google Scholar: Author Only Title Only Author and Title

de Lucas M, Davière J-M, Rodríguez-Falcón M, Pontin M, Iglesias-Pedraz JM, Lorrain S, Fankhauser C, Blázquez MA, Titarenko E, Prat S (2008) A molecular framework for light and gibberellin control of cell elongation. Nature 451: 480–484
Google Scholar: Author Only Title Only Author and Title

Merz D, Richter J, Gonneau M, Sanchez-Rodriguez C, Eder T, Sormani R, Martin M, Hématy K, Höfte H, Hauser M-T (2017) T-DNA alleles of the receptor kinase THESEUS1 with opposing effects on cell wall integrity signaling. Journal of Experimental Botany 68: 4583–4593
Google Scholar: Author Only Title Only Author and Title

Mielke S, Zimmer M, Meena MK, Dreos R, Stellmach H, Hause B, Voiniciuc C, Gasperini D (2021) Jasmonate biosynthesis arising from altered cell walls is prompted by turgor-driven mechanical compression. Science Advances 7: eabf0356
Google Scholar: Author Only Title Only Author and Title

Mølhøj M, Verma R, Reiter W-D (2004) The Biosynthesis of d-Galacturonate in Plants. Functional Cloning and Characterization of a Membrane-Anchored UDP-d-Glucuronate 4-Epimerase from Arabidopsis. Plant Physiology 135: 1221–1230
Google Scholar: Author Only Title Only Author and Title

Mouille G, Ralet M-C, Cavelier C, Eland C, Effroy D, Hématy K, McCartney L, Truong HN, Gaudon V, Thibault J-F (2007) Homogalacturonan synthesis in Arabidopsis thaliana requires a Golgi-localized protein with a putative methyltransferase domain. The Plant Journal 50: 605–614
Google Scholar: Author Only Title Only Author and Title

Nicol F, His I, Jauneau A, Vernhettes S, Canut H, Höfte H (1998) A plasma membrane-bound putative endo-1,4-β-d-glucanase is required for normal wall assembly and cell elongation in Arabidopsis. The EMBO Journal 17: 5563–5576
Google Scholar: Author Only Title Only Author and Title

Pfaffl MW (2001) A new mathematical model for relative quantification in real-time RT–PCR. Nucleic acids research 29: e45–e45
Google Scholar: Author Only Title Only Author and Title

Raggi S, Ferrarini A, Delledonne M, Dunand C, Ranocha P, De Lorenzo G, Cervone F, Ferrari S (2015) The Arabidopsis class III peroxidase AtPRX71 negatively regulates growth under physiological conditions and in response to cell wall damage. Plant physiology 169: 2513–2525
Google Scholar: Author Only Title Only Author and Title

Ray PM, Green PB, Cleland R (1972) Role of Turgor in Plant Cell Growth. Nature 239: 163–164
Google Scholar: Author Only Title Only Author and Title

Rayon C, Cabanes-Macheteau M, Loutelier-Bourhis C, Salliot-Maire I, Lemoine J, Reiter W-D, Lerouge P, Faye L (1999) Characterization of N-Glycans from Arabidopsis. Application to a Fucose-Deficient Mutant1. Plant Physiology 119: 725–734
Google Scholar: Author Only Title Only Author and Title

Reiter W-D, Chapple C, Somerville CR (1997) Mutants of Arabidopsis thaliana with altered cell wall polysaccharide composition. The Plant Journal 12: 335–345
Google Scholar: Author Only Title Only Author and Title

Reiter W-D, Chapple CC, Somerville CR (1993) Altered growth and cell walls in a fucose-deficient mutant of Arabidopsis. Science

261: 1032–1035
Google Scholar: Author Only Title Only Author and Title

Rizza A, Walia A, Lanquar V, Frommer WB, Jones AM (2017) In vivo gibberellin gradients visualized in rapidly elongating tissues. Nature Plants 3: 803–813
Google Scholar: Author Only Title Only Author and Title

Rouet M-A, Mathieu Y, Barbier-Brygoo H, Laurière C (2006) Characterization of active oxygen-producing proteins in response to hypo-osmolarity in tobacco and Arabidopsis cell suspensions: identification of a cell wall peroxidase. Journal of Experimental Botany 57: 1323–1332
Google Scholar: Author Only Title Only Author and Title

Rowe J, Grangé-Guermente M, Exposito-Rodriguez M, Wimalasekera R, Lenz MO, Shetty KN, Cutler SR, Jones AM (2023) Next-generation ABACUS biosensors reveal cellular ABA dynamics driving root growth at low aerial humidity. Nat Plants 9: 1103–1115
Google Scholar: Author Only Title Only Author and Title

Rowe JH, Rizza A, Jones AM (2022) Quantifying Phytohormones in Vivo with FRETFörster Resonance Energy Transfer (FRET)BiosensorsBiosensors and the FRETENATOR Analysis Toolset. In P Duque, D Szakonyi, eds, Environmental Responses in Plants: Methods and Protocols. Springer US, New York, NY, pp 239–253
Google Scholar: Author Only Title Only Author and Title

Rui Y, Dinneny JR (2020) A wall with integrity: Surveillance and maintenance of the plant cell wall under stress. New Phytologist 225: 1428–1439
Google Scholar: Author Only Title Only Author and Title

Shen X, Li Y, Pan Y, Zhong S (2016) Activation of HLS1 by Mechanical Stress via Ethylene-Stabilized EIN3 Is Crucial for Seedling Soil Emergence. Frontiers in Plant Science 7:
Google Scholar: Author Only Title Only Author and Title

Silk WK, Erickson RO (1978) Kinematics of Hypocotyl Curvature. American Journal of Botany 65: 310–319
Google Scholar: Author Only Title Only Author and Title

Sinclair SA, Larue C, Bonk L, Khan A, Castillo-Michel H, Stein RJ, Grolimund D, Begerow D, Neumann U, Haydon MJ, et al (2017) Etiolated Seedling Development Requires Repression of Photomorphogenesis by a Small Cell-Wall-Derived Dark Signal. Current Biology 27: 3403-3418.e7
Google Scholar: Author Only Title Only Author and Title

Široká J, Brunoni F, Pěnčík A, Mik V, Žukauskaitė A, Strnad M, Novák O, Floková K (2022) High-throughput interspecies profiling of acidic plant hormones using miniaturised sample processing. Plant Methods 18: 122
Google Scholar: Author Only Title Only Author and Title

Song S, Huang H, Gao H, Wang J, Wu D, Liu X, Yang S, Zhai Q, Li C, Qi T, et al (2014) Interaction between MYC2 and ETHYLENE INSENSITIVE3 Modulates Antagonism between Jasmonate and Ethylene Signaling in Arabidopsis. The Plant Cell 26: 263–279
Google Scholar: Author Only Title Only Author and Title

Sun T (2008) Gibberellin Metabolism, Perception and Signaling Pathways in Arabidopsis. Arabidopsis Book 6: e0103
Google Scholar: Author Only Title Only Author and Title

Vaahtera L, Schulz J, Hamann T (2019) Cell wall integrity maintenance during plant development and interaction with the environment. Nat Plants 5: 924–932.
Google Scholar: Author Only Title Only Author and Title

Verger S, Long Y, Boudaoud A, Hamant O (2018) A tension-adhesion feedback loop in plant epidermis. Elife 7: e34460
Google Scholar: Author Only Title Only Author and Title

Wasternack C, Hause B (2013) Jasmonates: biosynthesis, perception, signal transduction and action in plant stress response, growth and development. An update to the 2007 review in Annals of Botany. Annals of Botany 111: 1021–1058
Google Scholar: Author Only Title Only Author and Title

Willis L, Refahi Y, Wightman R, Landrein B, Teles J, Huang KC, Meyerowitz EM, Jönsson H (2016) Cell size and growth regulation in the Arabidopsis thaliana apical stem cell niche. Proceedings of the National Academy of Sciences 113: E8238–E8246
Google Scholar: Author Only Title Only Author and Title

Wolf S, Hématy K, Höfte H (2012) Growth Control and Cell Wall Signaling in Plants. Annual Review of Plant Biology 63: 381–407
Google Scholar: Author Only Title Only Author and Title

Zhang B, Holmlund M, Lorrain S, Norberg M, Bakó L, Fankhauser C, Nilsson O (2017) BLADE-ON-PETIOLE proteins act in an E3 ubiquitin ligase complex to regulate PHYTOCHROME INTERACTING FACTOR 4 abundance. eLife 6: e26759
Google Scholar: Author Only Title Only Author and Title

Zhang X, Ji Y, Xue C, Ma H, Xi Y, Huang P, Wang H, An F, Li B, Wang Y (2018) Integrated regulation of apical hook development by

transcriptional coupling of EIN3/EIL1 and PIFs in Arabidopsis. The Plant Cell 30: 1971–1988
Google Scholar: Author Only Title Only Author and Title

Zhang X, Zhu Z, An F, Hao D, Li P, Song J, Yi C, Guo H (2014) Jasmonate-Activated MYC2 Represses ETHYLENE INSENSITIVE3 Activity to Antagonize Ethylene-Promoted Apical Hook Formation in Arabidopsis. The Plant Cell 26: 1105–1117
Google Scholar: Author Only Title Only Author and Title